ESD-TR-66-199

Technical Report

416

F. I. Sheftman

Experimental Study of Subreflector Support Structures in a Cassegrainian Antenna

23 September 1966

Prepared under Electronic Systems Division Contract AF 19(628)-5167 by

Lincoln Laboratory
MASSACHUSETTS INSTITUTE OF TECHNOLOGY
Lexington, Massachusetts

The work reported in this document was performed at Lincoln Laboratory, a center for research operated by Massachusetts Institute of Technology, with the support of the U.S. Air Force under Contract AF 19(628)-5167.

Distribution of this document is unlimited.

MASSACHUSETTS INSTITUTE OF TECHNOLOGY

LINCOLN LABORATORY

EXPERIMENTAL STUDY OF SUBREFLECTOR SUPPORT STRUCTURES IN A CASSEGRAINIAN ANTENNA

F. I. SHEFTMAN

Group 46

TECHNICAL REPORT 416

23 SEPTEMBER 1966

LEXINGTON MASSACHUSETTS

ABSTRACT

The effects of various support structures on the radiation patterns of a Cassegrainian antenna have been investigated experimentally. Detailed two-dimensional contour plots of the wide-angle radiation are presented primarily for support member dimensions up to about one wavelength. We show that the disturbing effects decrease rapidly for perpendicular polarization when the dimensions are decreased below $\lambda/2$. Furthermore, the on-axis geometrical shadowing due to the support members does not give the correct level and shape of the wide-angle radiation. Account must be taken of the polarization and orientation of the members relative to the antenna axis. The performance of dielectric members is shown to be generally poorer than that of metallic members. The alternative of supporting the subreflector with a thin-wall axial dielectric cylinder is shown to be electrically acceptable for thicknesses of the order of 0.01λ. The data presented should be useful in designing and evaluating various types of support structures for Cassegrainian and front-fed reflectors.

Accepted for the Air Force
Franklin C. Hudson
Chief, Lincoln Laboratory Office

CONTENTS

EXPERIMENTAL STUDY OF SUBREFLECTOR SUPPORT STRUCTURES IN A CASSEGRAINIAN ANTENNA

I. INTRODUCTION

In most applications of reflector-type antennas, some form of mechanical structure is required to support the feed or subreflector. Such a structure unavoidably shadows, or blocks, a portion of the aperture and consequently degrades the performance of the antenna.

This problem has been discussed in the literature in a rather approximate fashion.[1-4] The usual approach consists of projecting the subreflector and support members geometrically upon the aperture. The long and narrow blocked areas due to typical support members produce fan beams perpendicular to the members, while the subreflector shadow produces a broad circular pattern. These radiation patterns are taken to be out of phase and are added to the pattern of the undisturbed aperture. Certain correction factors may be applied, so that the location of the shadowed region is properly weighted for a tapered aperture illumination. The composite pattern then represents the radiation of the shadowed aperture.

This procedure implies that the support structure members are large (optical approximation) and absorb, rather than scatter, the energy incident upon them. It yields a reasonable estimate of the loss (or gain) of effective area and the increase in level of the close-in sidelobes. However, the average level and angular location of the wide-angle radiation can be estimated rather imprecisely, since no account is taken of the scattered or reradiated energy, nor of the orientation of the members and the change in shadowing for off-axis angles. Further difficulty is encountered when nonoptical blockage occurs, i.e., when the dimensions of the support members are less than a half wavelength. In that case, the polarization of the incident field relative to the support members is more important than the geometrical shadowing.

Since an exact calculation of the effects of subreflector supports is usually prohibitively involved, an experimental approach was chosen which, although tedious and time-consuming, is capable of producing complete and reliable data in a carefully arranged setup. This detailed information is essential for evaluating the interference susceptibility and noise temperature of an antenna, both of which are largely determined by the wide-angle radiation. It is also expected to be helpful in choosing and designing suitable support structures for Cassegrainian as well as front-fed reflectors.

The experimental work began with the calibration of the test antenna at the site in order to determine whether the residual sidelobe level under conditions of minimum blockage was sufficiently low. Next, the effects of single support members in a simplified geometry were studied to determine polarization effects. Following this, quadripods and tripods in various orientations were tested. Metallic and dielectric members in a representative tripod configuration

were compared. Finally, a thin-wall axial dielectric cylinder for supporting the subreflector was investigated. All experimental data were taken at 9 Gcps.

II. TEST PROCEDURE AND EXPERIMENTAL SETUP

Conventional principal-plane patterns as well as two-dimensional "contour" plots were taken to provide an adequate picture of the radiation in all significant directions. A Scientific Atlanta Radiation Distribution Printer proved a very useful tool in obtaining the contour plots. To utilize this printer, the antenna was mounted on a conventional elevation-on-azimuth pedestal and rotated ±45° in azimuth for each elevation angle of interest. The printer typed a number corresponding to the signal level in decibels for every 0.5° increment of azimuth rotation. The resulting plot was somewhat similar to a television scan and was converted to a more useful representation by drawing contour lines at 5-dB intervals. Frequently, much detail was omitted in order to avoid excessive cluttering of the plots with unimportant "holes" or minima. Isolated high spots are shown, of course, since they are very definitely of interest. As given, the contour plots represent a transmit view, which is the mirror image of the radiation seen by a remote observer in front of the antenna.

Before we describe the investigation of the effects of various support structures, it is interesting to examine the radiation patterns of typical antennas. Figure 1 is a contour plot for the sum channel of a conventional four-horn monopulse Cassegrainian antenna. The main reflector is a paraboloid with a diameter of 110 inches and an f/d ratio of 0.25. The subreflector support is a tripod similar to that shown in Fig. 20, except that the diameter of the members tapers at each end and has a maximum value of 1.52λ. The very high and extensive spillover energy of the primary feed is quite evident. The rather irregular appearance of the radiation in the central portion is caused by the support structure, but the specific nature of the disturbance is obscured by the high spillover level.

In Fig. 1, the region 0 to 40 dB below the peak of the main beam is indicated by conventional contour lines. The unmarked lines enclosing small areas have values corresponding to the higher of the two adjacent contour lines. For clarity, the region 40 to 45 dB below the peak of the main beam is lightly shaded; the region 45 to 50 dB below the peak is indicated by a medium-dark pattern; and the region below 50 dB is identified by a dark pattern.

Use of a single-horn Cassegrainian feed reduces the spillover substantially, as seen in Figs. 2(a) and (b). These principal-plane patterns are sufficient to illustrate the still high spillover level due to the E-plane sidelobes of the conventional feedhorn. Near the main beam, 30-dB attenuation is inserted in the transmission line to achieve a 70-dB dynamic range.

It is now evident that a still "cleaner" primary feed is desirable in order not to obscure the effects of the subreflector support structure. We felt that a feed aperture comparable in size with the subreflector would have better spillover characteristics. This was based, in part, on the fact that the spillover level is determined essentially by the sidelobe level of the primary feed; a larger feed of proper design should have lower far-out sidelobes. Also, since the subreflector would be in the near field of the feed aperture, we would have a better approximation of the optical region which, theoretically, should produce no spillover.

To avoid excessive feedhorn length, a 12-inch lens fed by a multimode horn with a square aperture* (3.65 × 3.65 inches) was chosen for the experimental setup. The polystyrene lens

*Designed by W. D. Fitzgerald of this Laboratory.

was a simple unmatched design with a hyperboloidal refracting surface and a 12-inch focal length. The horn-lens feed was mounted in a thin-wall fiberglass cylinder lined with absorbing material (Fig. 3). This arrangement resulted in good illumination of the subreflector as well as low spillover due to the horn. It also permitted the substitution of a conventional feedhorn to check on the effects of the higher secondary cross polarization resulting from the multimode horn (– 25 dB). The conventional feedhorn, which has no inherent cross polarization, produced secondary cross-polarized energy 35 dB below the main beam. In both cases, this energy dropped rapidly to low levels a few degrees away. A further check with a typical support structure showed similar radiation patterns for the two horns. Since the multimode horn had considerably higher efficiency, it was used for all the measurements presented in this report.

Although a paraboloidal subreflector is desirable when used in the near field of the feed, good patterns were obtained by appropriate focusing of the hyperboloidal subreflector used for taking the data presented in Figs. 1 and 2. About 0.2 dB more gain and somewhat better patterns near the main beam were obtained with a paraboloidal subreflector, but the far-out radiation was quite similar. The maximum gain was about 0.4 dB lower than that of the conventional Cassegrainian pattern of Fig. 2. However, the greater illumination taper of the horn-lens feed produced a wider beam and was partly responsible for the lower gain. Since gain and beamwidth were of secondary interest in this investigation, the hyperboloidal subreflector was used in obtaining all subsequent data for reasons of convenience. Incidentally, this subreflector was slightly oversize, but this was probably beneficial.[5] In general, our results agree with the published data of Hogg and Semplak[6] for the near-field Cassegrainian antenna.

The test site was the 2000-foot Lincoln Laboratory ground-reflection range. The antenna was located inside an absorber-lined 20-foot test cubicle (Fig. 4). Limitations of the absorbing material and cubicle design were evident when radiation patterns were taken with the minimum possible blockage. To accomplish this, the subreflector was initially supported by very thin dacron strings (Fig. 5). Wooden outriggers were used to provide longitudinal stability. Although dacron has low-stretch properties, the setup was not sufficiently stable over a period of several weeks, so piano wires 1/32 inch in diameter were eventually substituted. The effect of the wires on the patterns was very small, although still discernible. Rigidity and stability with this arrangement were remarkably good. Most of the data were taken with dummy support members, the subreflector being held in place by the wires.

In general, the dummy members were made of wood and covered with aluminum foil. Consequently, the relevant data are directly applicable only to solid metallic structures. Members of circular and rectangular cross sections were investigated, the latter being oriented for minimum blockage.

The typical support structure (or spider) has long, thin members often called spars or struts. A given structure, such as a tripod or a quadripod, may be oriented in three possible ways, although not all three are practical for the same reflector. Figure 6(a) illustrates an arrangement which we shall call, descriptively, "spars inside the aperture." The point of attachment to the main reflector is about halfway from the vertex to the outside rim. Figure 6(b) is an arrangement termed "spars outside the aperture." The point of attachment is at the outside rim. Figure 6(c) is a special case of Fig. 6(b) and is practical for deep dishes with f/d ratios less than 0.25. It is identified as "spars at the aperture" and is treated separately because of its peculiar behavior. All three configurations were easily implemented in the test dish, since

the subreflector relied only on the wires for its support. There was no contact between the spars and the subreflector in most cases. In the geometries of Figs. 6(a) and (b), the spars were of such length as to form an angle of approximately 45° with the dish axis.

III. EXPERIMENTAL RESULTS

A. Calibration Run

In a Cassegrainian geometry, it is possible to isolate the primary feed pattern from the secondary pattern by the simple expedient of replacing the subreflector with an efficient absorber of microwave energy. This makes it easier to identify the far-out radiation as either spillover energy, site-generated reflections, or secondary sidelobes. The patterns of Figs. 7(a) and (b) were taken with the subreflector supported by wires only. It is seen that the sidelobes of the 12-inch lens feed (dashed curve) may well be taken as the approximate upper limit of the forward spillover (solid curve) at far-out angles. Since this is a highly directive antenna, the spillover pattern is also expected to be the upper limit on the envelope of the secondary pattern at wide angles. This is not strictly the case here, and the appearance of the sidelobes would suggest that they are the result of site reflections. However, the residual level is well below isotropic, and any observed increase in sidelobes due to the subreflector supports should be reliable to this level, at least in the principal planes.

Figure 8 is one-half of a symmetrical contour plot taken when the subreflector was supported by wires only. It is quite similar to that for the case of dacron strings, but is somewhat more irregular. We can see that the isotropic level is reached at angles of 10° to 15° from the main beam.

A detailed picture of the spillover is given by the contour plot of Fig. 9, which is merely the arrangement of Fig. 8 with the subreflector covered by a good microwave absorber. This gives a good approximation of the energy spilled over by the feed at all angles. Comparison of the two figures casts some doubt about the origin of some of the sidelobes of Fig. 8. For example, it is not clear in Fig. 8 whether the annular lobe about 32° away from the main beam is genuine or, more likely, a result of the finite reflectivity of the test cubicle. However, the maximum level of this lobe remains below isotropic, and all future data may be considered reliable approximately to this level.

B. Effects of Single Spar at Aperture

For the particular case of the deep test dish, it was practical to support the subreflector by members located at the aperture [Fig. 6(c)]. This arrangement probably presents the simplest blocking geometry. A variation of this involves one substantial member braced by guy cables. It would appear that the large member should be less troublesome if oriented normal to the dominant polarization. This proves to be very important for dimensions smaller than a half wavelength.

A contour plot for a typical geometry is shown in Fig. 10. The most notable feature is the long vertical lobe perpendicular to the rectangular spar. The width of 0.77λ apparently produces little directivity in the E-plane. The sidelobe level in the horizontal plane has also increased, but to a much smaller extent.

At this point in the measurement program, it became interesting to determine the effect of the size of the spars. To accomplish this quickly, only principal-plane patterns were taken

perpendicular to the members. Figure 11(a) shows the results for polarization perpendicular to the spar. The geometry is that of Fig. 10 rotated 90°. The close-in sidelobes were found to increase monotonically with spar size for both rectangular and circular members. The envelope of the far-out sidelobes exhibited lobing roughly consistent with the behavior of a uniformly illuminated line source having a width equal to that of the spar. In general, the minima occurred somewhat farther out for circular members, while the maxima were somewhat lower.

No lobing was observed in the case of parallel polarization, as seen in Fig. 11(b). Members having the same widths produce a substantially greater effect here than in the case of perpendicular polarization. In addition, there is little difference between the measured patterns of the $\lambda/2$ and the λ-wide spars at far-out angles. Obviously, based on shadowed area, the calculated curves have little relevance here. As a rule, there were no important changes as the spar depth was increased moderately. Circular members generated spar lobes which decreased somewhat more slowly at far-out angles than did rectangular members of equal width.

A direct comparison of the effects of polarization is given in Fig. 11(c). To avoid confusion due to excessive detail, only the envelopes of the sidelobes for the no-spar curves are shown. These patterns, together with other data (not shown) for narrower spars, demonstrate that the effective shadow area decreases much more slowly with spar width for parallel than for perpendicular polarization. The width at which this becomes noticeable is somewhat less than $\lambda/2$ for rectangular spars and somewhat greater than $\lambda/2$ for circular spars.

Since very thin spars are of no practical interest, except in the form of guy cables, a few measurements were made on the effects of wires at the aperture. For parallel polarization, it is estimated (by extrapolation of the data) that the diameter should be under 0.04λ, and, for perpendicular polarization, under 0.15λ for negligible effect on the pattern of the test antenna. These results are in agreement with published data for the total scattering cross section of infinitely long conducting cylinders.[7] At very small diameters, the calculated effective cross section for parallel polarization is much greater than for perpendicular polarization. There are no resonances as the cross section increases with cylinder size. Only when the diameter is over a wavelength in size do the cross-section areas approach equality, in which case they are equal to the physical size (optical approximation).

C. Principal-Plane Quadripod

For the purposes of comparison with other configurations, a contour plot for the principal-plane spars at the aperture is presented in Fig. 12. The large vertical lobe of Fig. 10 is considerably lower here, since the width of the horizontal spar (perpendicular polarization) is less than $\lambda/2$. However, the vertical spar (parallel polarization) produces a very prominent lobe in the horizontal plane.

When spars having similar dimensions are installed inside the aperture, the contour plot of Fig. 13 is obtained. The horizontal spar lobe (parallel polarization) is very substantial, but it does not extend as far out as in Fig. 12. This can be explained, in part, by the fact that the shadowed area is wider and the associated fan beam is more directive. The curvature of the fan beam and its bifurcation at wide angles are more pronounced in Figs. 14 and 15 and will be explained in the following discussion.

The third arrangement of spars is outside the aperture, and the appropriate contour is given in Fig. 14(a). Greater regularity and a more pronounced bifurcation of the spar lobes

are apparent. This arrangement has the same geometrical on-axis shadowing as the case for spars at the aperture (Fig. 12). However, the appearance of the spar lobes is quite dissimilar. The horizontal spars (perpendicular polarization) are sufficiently thin, so they have no major effect here, the observed spar lobes being due primarily to the vertical members. When the spars are sufficiently wide, they all generate fan beams, as seen in Fig. 14(b).

The curvature and bifurcation of the spar lobes can be explained in several ways. Taking the aperture as a receiver, it is apparent that the shadowing due to the spars varies as a function of off-axis arrival angles. Figure 15(a-d) is a series of photographs of a model illustrating this effect. Since the long and narrow shadow regions generate fan beams (spar lobes) perpendicular to their long dimensions, curvature sets in as the blocked areas move out of the principal planes.

An alternative, and perhaps more satisfying, approach consists of a transmit view requiring a three-dimensional geometry. Any spar not parallel to the aperture plane is replaced by a line source having the same orientation and a progressive phase delay determined by that orientation. Instead of a fan beam associated with an in-phase line source, we now have a conical beam. This produces the curvature observed in Figs. 13 and 14. Inspection shows that this curvature is consistent with a line source inclined 45° from the antenna axis and phased to radiate in the forward direction. The bifurcation, of course, is due to the fact that there are two differently oriented members in each of the planes containing the spars.

Comparison of the three configurations of Figs. 12 through 14 shows that the case of spars at the aperture (Fig. 12) is least desirable. This is due to the fact that the spars retain the same relationship to the E-field at all angles in the principal planes. For example, a vertical spar produces its major effect in the horizontal plane, and it remains vertical at all azimuth angles. Similarly, a horizontal spar produces its effect in the vertical plane, and it remains horizontal for all elevation angles.

D. Diagonal Quadripod

The three configurations of Fig. 6 were next tested with diagonal spars having the same dimensions as those given in Sec. III-C. Figure 16(a) is a contour plot for the case of diagonal spars at the aperture; Figs. 17(a) and 18(a) are plots of similar size spars inside and outside the aperture, respectively. As before, the inside case shows the greater irregularity, and the outside case is the more desirable, although by a small margin. The effects of more massive spars are shown in Figs. 16(b), 17(b), and 18(b).

An increase in spar thickness is normally expected to reduce the wide-angle radiation and raise the close-in sidelobes. We found that rounding-off the corners, or tapering the cross section, of rectangular spars reduces slightly the level of the spar lobes. Substitution of a circular member of equal shadowing cross section for a rectangular one lowers somewhat the close-in sidelobes, but it also lowers the directivity of the spar lobes, as discussed previously in Sec. III-B. This may not be an improvement, as seen in Fig. 19, where the spar diameter is actually less than the minimum dimension of the rectangular members of Fig. 16(b). However, this result cannot be generalized. For example, when the rectangular spars of Fig. 17(a) were replaced by circular spars with a diameter equal to the narrow dimension, a cleaner and better contour plot (not shown) was obtained. With rectangular spars, no interesting effects were observed when the depth or width were odd or even multiples of $\lambda/2$. Similarly, with circular

members, no resonant effects were found when the diameter assumed these dimensions. In passing, it may be pointed out that conventional principal-plane patterns do not show the spar lobes of a diagonal structure. Moreover, under some conditions a diagonal structure may actually decrease substantially the first sidelobes in the principal planes.

E. Tripod

The quadripod support structures discussed thus far are symmetrical both electrically and mechanically. The quadripod in the principal planes is particularly convenient for experimental work because of ease of adjustment in these planes. Another frequently used structure, the tripod, is neither symmetrical electrically nor as convenient to adjust in the conventional setup, but it is quite desirable from a structural point of view. Only cylindrical members were used in the tripod configuration of this study.

Figure 20(a) shows the complete contour plot for the tripod inside the aperture. The round members of substantial size that are used here produce considerable specular scattering in addition to the perpendicular fan beams. The vertical spar produces the two horizontal lobes which curve downward with increasing off-axis angle. It also scatters energy off its inner side, as seen in the lower central portion of the figure. The two lower spars behave in a similar fashion and generate the other lobes. Since they are not parallel to the incident field, their effect is not as great. To show the relative effects and to help identify the source of the spar lobes, a contour plot with only the upper member in place is presented in Fig. 20(b).

The contour plot for the tripod outside the aperture is presented in Fig. 21. As expected, the pattern is more regular and the spar lobes are well defined. Again, it is apparent that principal-plane patterns do not reveal the true extent of the spar lobes.

A tripod configuration with dielectric members gave interesting results. The geometry is similar to that of Fig. 20. Tubes of phenolic laminate (NEMA grade LE, natural color) having a 1.24-λ o.d. and a 1.05-λ i.d. were used. This material has high loss and high dielectric constant at the operating frequency. Figure 22 shows substantially more extensive far-out sidelobes than for the metallic spars. Tests with other dielectric materials of various sizes showed that they generally cause greater gain loss than metallic members of the same size. Hogg and Semplak[6] found that greater noise temperature results from the use of fiberglass supports. Our measurements show that this is to be expected from the extensive far-out radiation. Furthermore, we measured a gain loss of 0.75 dB due to the dielectric spars, compared with a loss of 0.5 dB with metallic spars of the same size and orientation. As expected, the metallic tripod outside the aperture caused a smaller gain loss (0.3 dB). The smaller size of the quadripod members in the preceding cases caused a smaller gain loss (a few tenths of a decibel), which was difficult to measure accurately and consistently with the available equipment. In general, the gain loss calculated on the basis of area blockage was much too low for metallic members.

F. Dielectric Cylinder

An alternative method of supporting the subreflector of a Cassegrainian antenna was suggested by J. G. Jelatis of this Laboratory. It involves the use of a thin-wall dielectric cylinder, as shown in Fig. 23. Transverse rigidity is provided by thin dacron strings. This scheme is similar to one investigated by Hogg and Semplak,[6] except that sufficient wall thickness was to be used to make pressurization unnecessary. As seen previously, very thin metallic guy wires can be used, if desired, with negligible electrical disturbance.

The basic problem here is the large variation in incident angles at the cylinder wall for rays reflected from the subreflector. The effect is minimized by using a material with the smallest possible dielectric constant and thickness. Low loss tangent and high mechanical strength are also desirable. Practical considerations led to the final choice of glass-epoxy laminates, NEMA grades G-10 and G-11. This material, popularly called fiberglass, has a relatively high dielectric constant. However, it is probably the strongest of the laminates suitable for this application and can therefore have the smallest thickness. Several samples from different manufacturers and of different thicknesses were tried, as well as other glass laminates having lower dielectric constants.

A G-10 cylinder with a wall thickness of 0.01 λ (0.013 inch) had negligible effect on the peak gain and on the E-plane pattern. However, in the H-plane there was an increase in sidelobe level of up to 5 dB at some intermediate angles, the level at close-in and far-out angles being essentially unchanged.

A thicker cylinder (G-11) with a wall thickness of 0.0175 λ (0.023 inch) produced a gain loss of about 0.25 dB despite use of an E-H tuner to eliminate any mismatch losses. No benefit was derived from refocusing the subreflector for this wall thickness. There was an even larger increase in the level of the intermediate H-plane sidelobes, the close-in and far-out level remaining unchanged. As before, there was only a minor change in the level of the E-plane sidelobes. A contour plot of the 110-inch dish with this cylinder is shown in Fig. 24.

The use of thicker material resulted in additional gain loss and an increase in the first sidelobe level. Part of this gain loss apparently was due to phase error, and it could be offset slightly by refocusing the subreflector. In general, the overall performance became degraded rather rapidly as the thickness was increased.

IV. CONCLUSIONS

Experimentally determined two-dimensional radiation patterns have been presented for a Cassegrainian antenna with various types of subreflector support structures. The data were shown to be reliable to the isotropic level over an angular sector greater than 100×100 beamwidths. This information should be helpful to the designer and user of reflector antennas. Only solid metallic support members with dimensions up to about λ are treated. No data are given for perforated, shaped, or absorber-covered members.

It is difficult to make precise estimates of the effects of typical support structures. Various parameters such as width, length, material, orientation, and polarization interact in a complex fashion. We found that the geometrically shadowed area in the on-axis case is not an adequate indicator of the shape and magnitude of the sidelobes generated by the support members. The migration of the shadowed area with increasing off-axis angles must be considered, or, more rigorously, the three-dimensional line sources corresponding to the members.

Appreciable effects occur for parallel, but not for perpendicular, polarization when the dimensions are smaller than a half wavelength. In general, the effects at close-in angles increase smoothly with the size of conducting support members. At far-out angles, lobing occurs in the envelope of the fan beam associated with a typical member that is perpendicular to the incident wave. Moderate increases in the depth of rectangular members have little effect. The directivity of the fan beam associated with a round member is slightly less than that of a rectangular member of equal width.

Perhaps the most favorable structure employing solid metallic members consists of narrow diagonal spars fastened to the reflector's rim and forming a moderate acute angle with its axis.

Dielectric support members were shown to be capable of producing considerably poorer electrical performance than metallic members of identical size and orientation. Another type of dielectric structure, the thin-wall axial cylinder, caused negligible gain loss and small increase in sidelobes, provided the wall thickness did not exceed 0.01 λ. Doubling the thickness caused a gain loss greater than 0.25 dB and a moderate increase in sidelobes. The thinner cylinder may be adequate structurally for some applications, but its contribution to the noise temperature of the antenna due to dielectric loss, though probably small, must be determined by direct measurement.

ACKNOWLEDGMENTS

The author wishes to thank Dr. K. J. Keeping, Dr. J. Ruze, and W. D. Fitzgerald for helpful discussions and for reading the manuscript. E. F. Pelrine assisted in the experimental work and in drawing the contour plots.

REFERENCES

1. S. Silver, Microwave Antenna Theory and Design (McGraw-Hill, New York, 1949), p. 190.
2. H. Jasik, ed., Antenna Engineering Handbook (McGraw-Hill, New York, 1961), p. 12.
3. C. L. Gray, "Estimating the Effect of Feed Support Member Blocking on Antenna Gain and Sidelobe Level," Microwave J. 7, No. 3, 88 (March 1964).
4. E. Everhart and J. W. Kantorski, "Diffraction Patterns Produced by Obstructions in Reflecting Telescopes of Modest Size," Astron. J. 64, 455 (1959).
5. P. D. Potter, "A Simple Beamshaping Device for Cassegrainian Antennas," Technical Report 32-214, Jet Propulsion Laboratory, California Institute of Technology (31 January 1962).
6. D. C. Hogg and R. A. Semplak, "An Experimental Study of Near-Field Cassegrainian Antennas," Bell System Tech. J. 43, 2677 (1964).
7. R. W. P. King and T. S. Wu, The Scattering and Diffraction of Waves (Harvard University Press, Cambridge, 1959), p. 66.

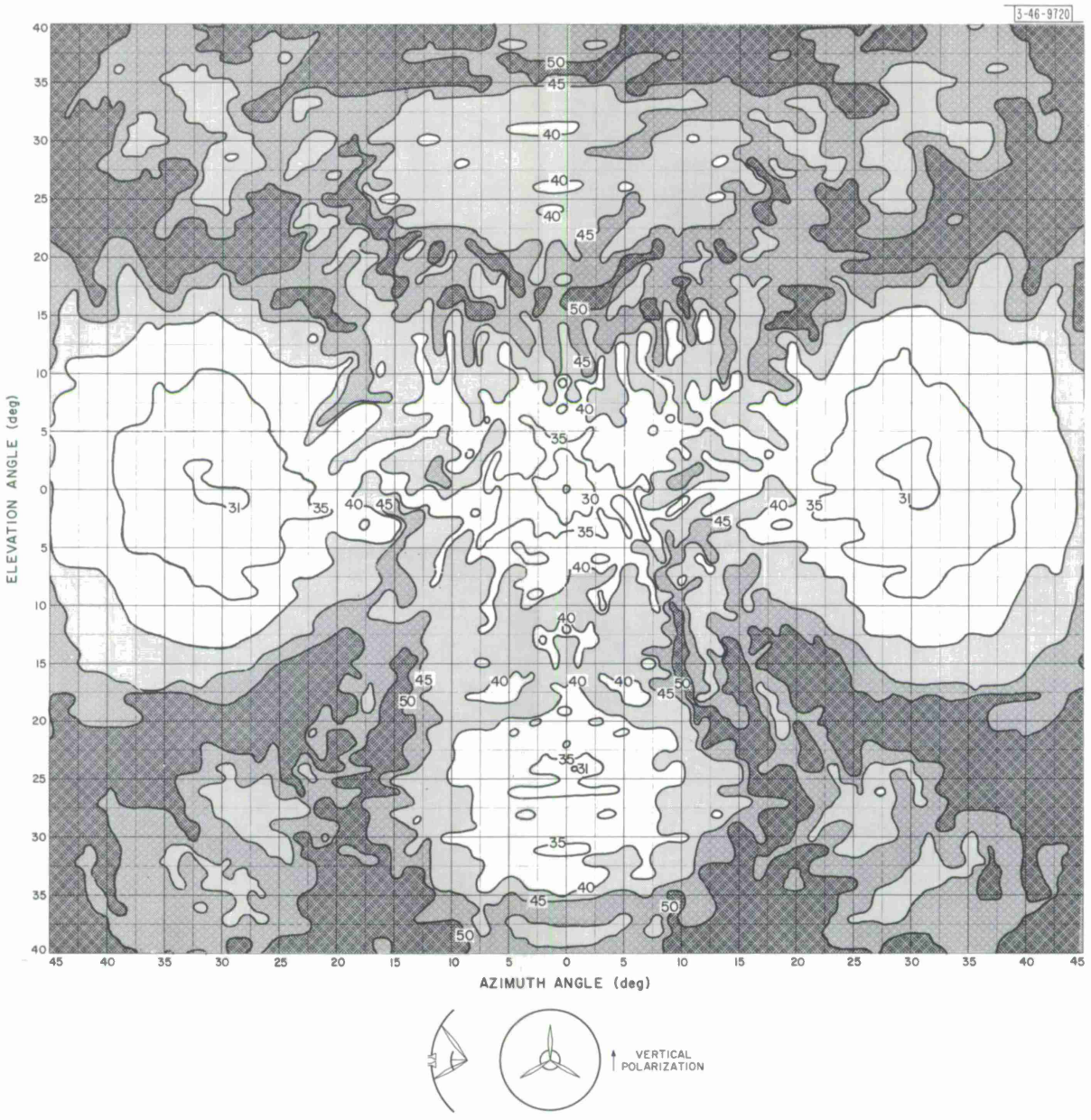

Fig. 1. Contour plot for 110-inch Cassegrainian dish with conventional four-horn monopulse feed.

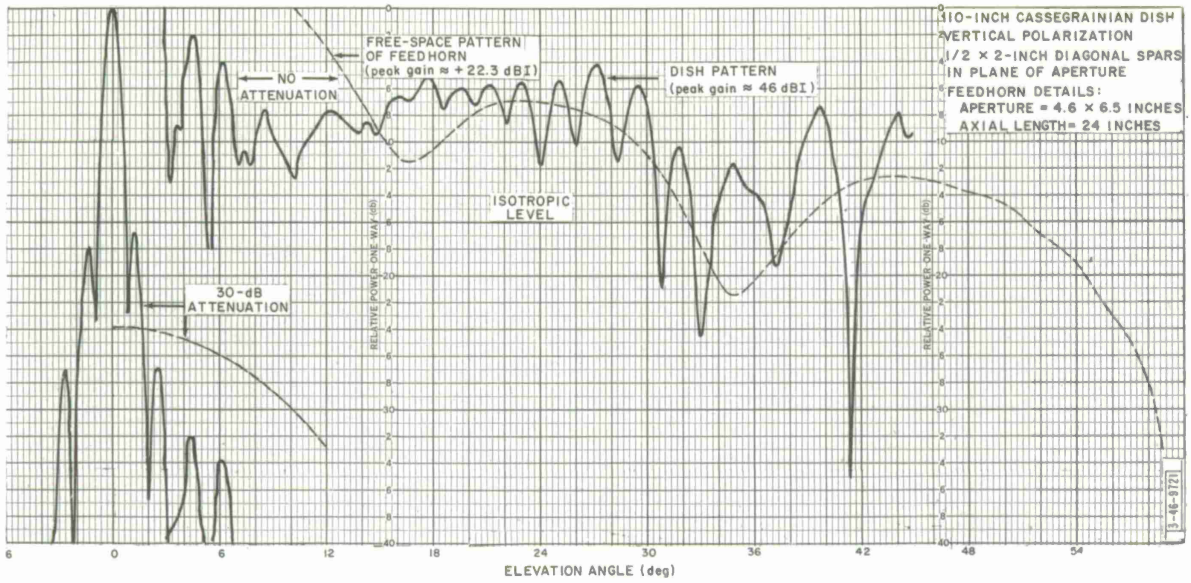

Fig. 2(a). Conventional Cassegrainian pattern (E-plane) with single-horn feed.

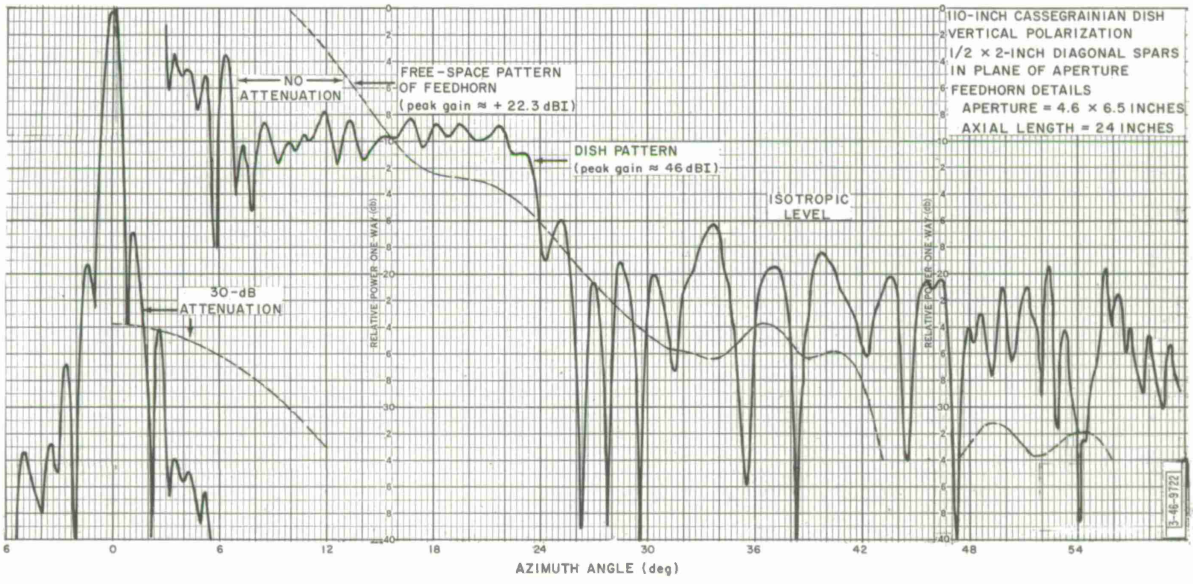

Fig. 2(b). Conventional Cassegrainian pattern (H-plane) with single-horn feed.

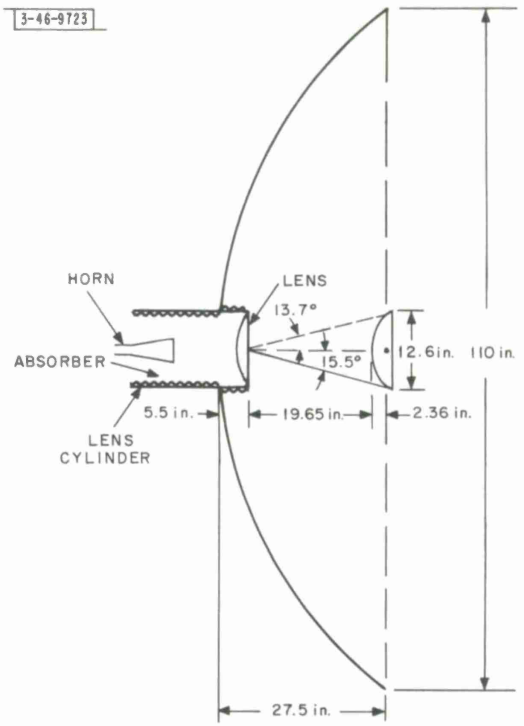

Fig. 3. Diagram of 110-inch dish and feed arrangement.

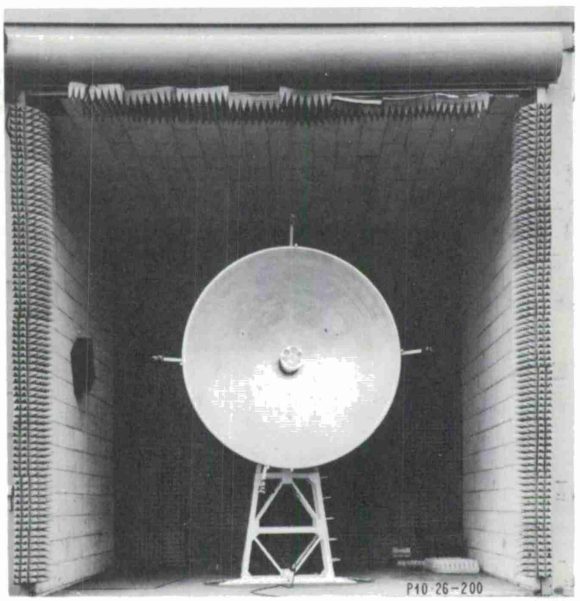

Fig. 4. 110-inch dish in test cubicle.

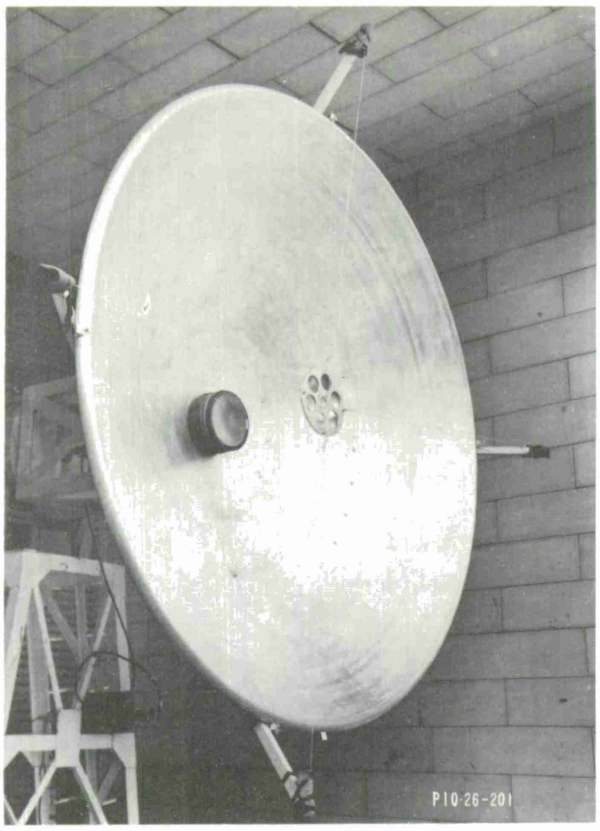

Fig. 5. Close-up of 110-inch dish with subreflector supported by dacron strings.

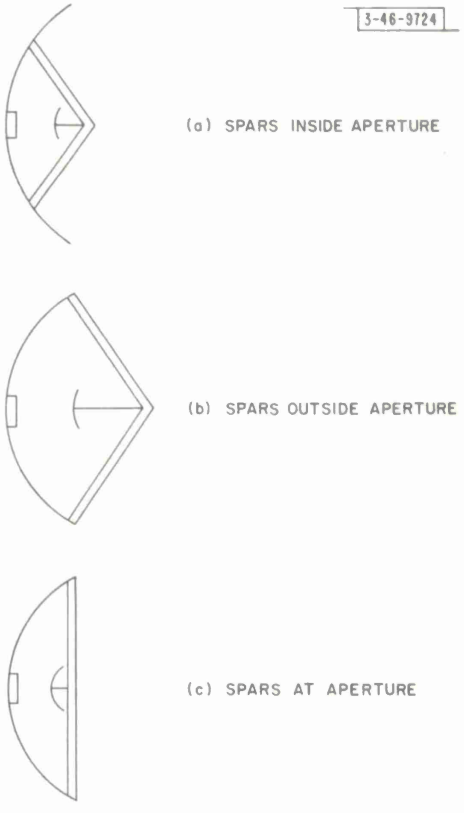

Fig. 6. Three configurations for a support structure.

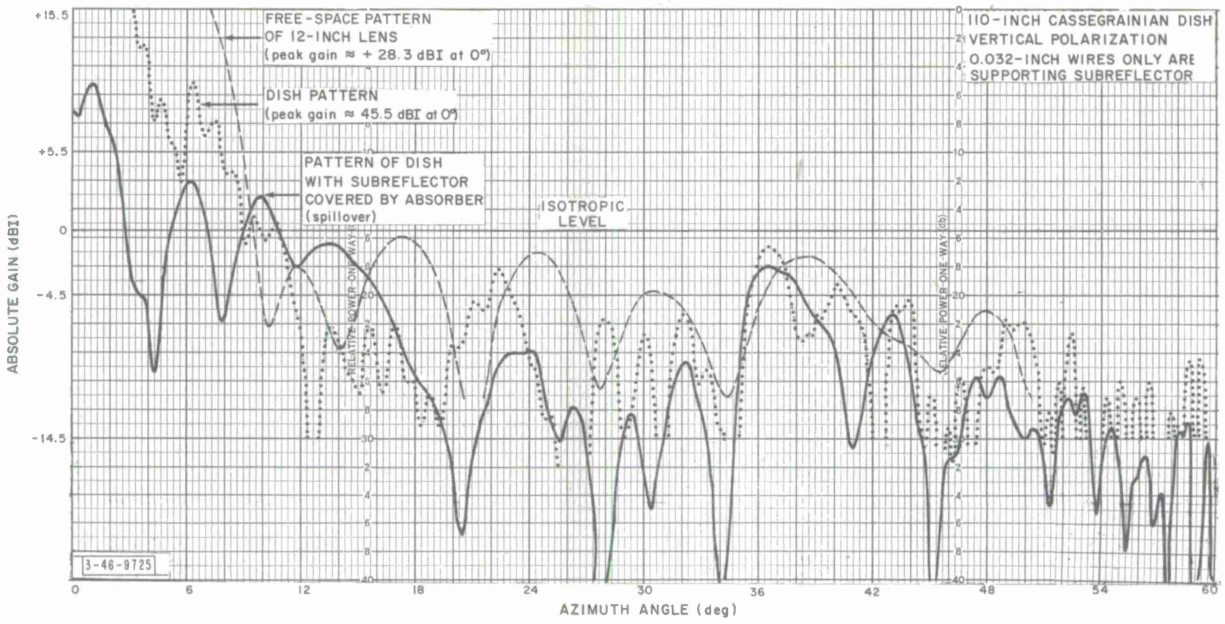

(a) H-plane pattern.

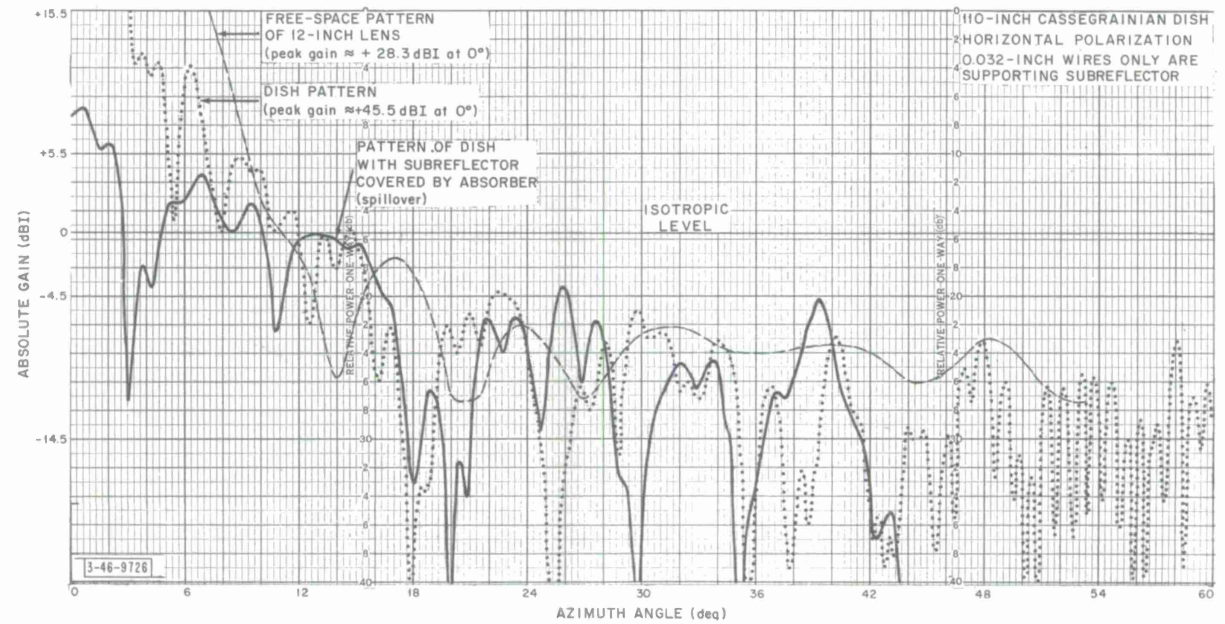

(b) E-plane pattern.

Fig. 7. Antenna and site evaluation.

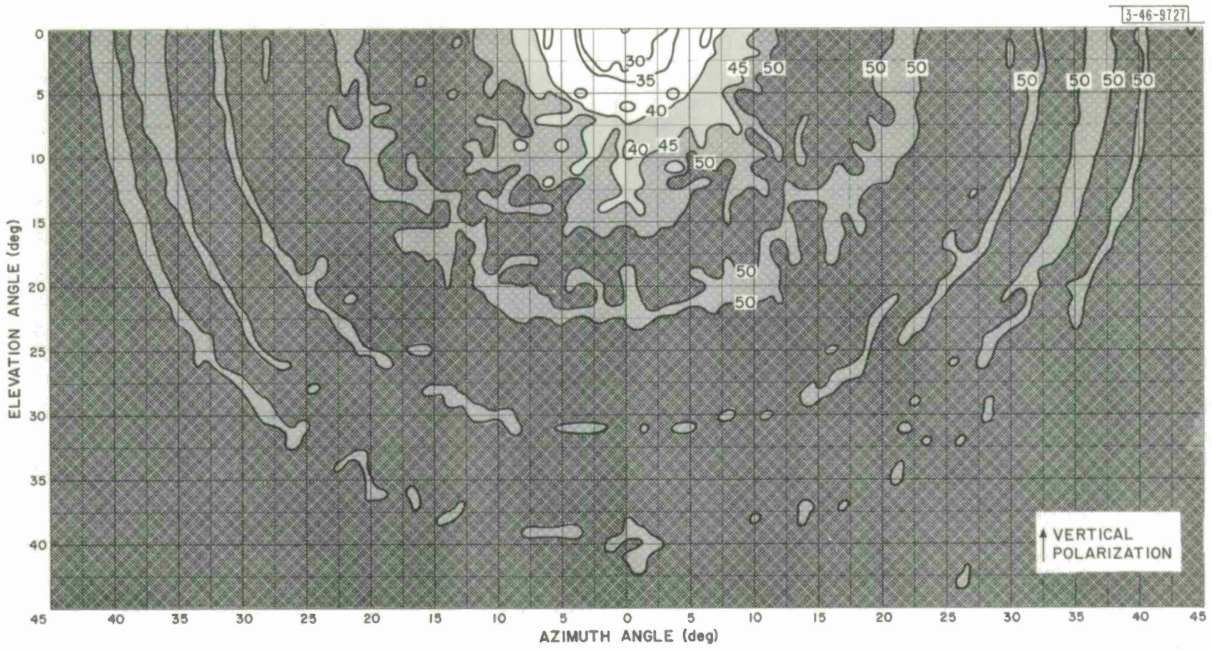

Fig. 8. Contour plot for 110-inch Cassegrainian dish with subreflector supported by 1/32-inch piano wires.

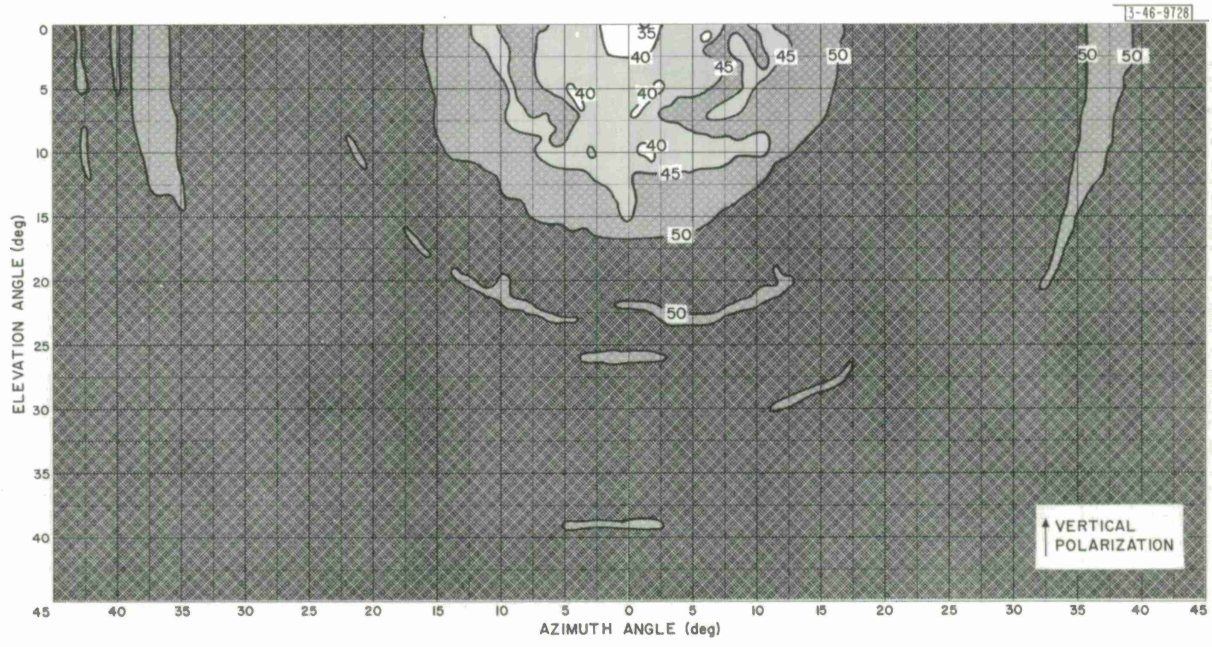

Fig. 9. Contour plot for 110-inch Cassegrainian dish with absorber on subreflector (spillover contour).

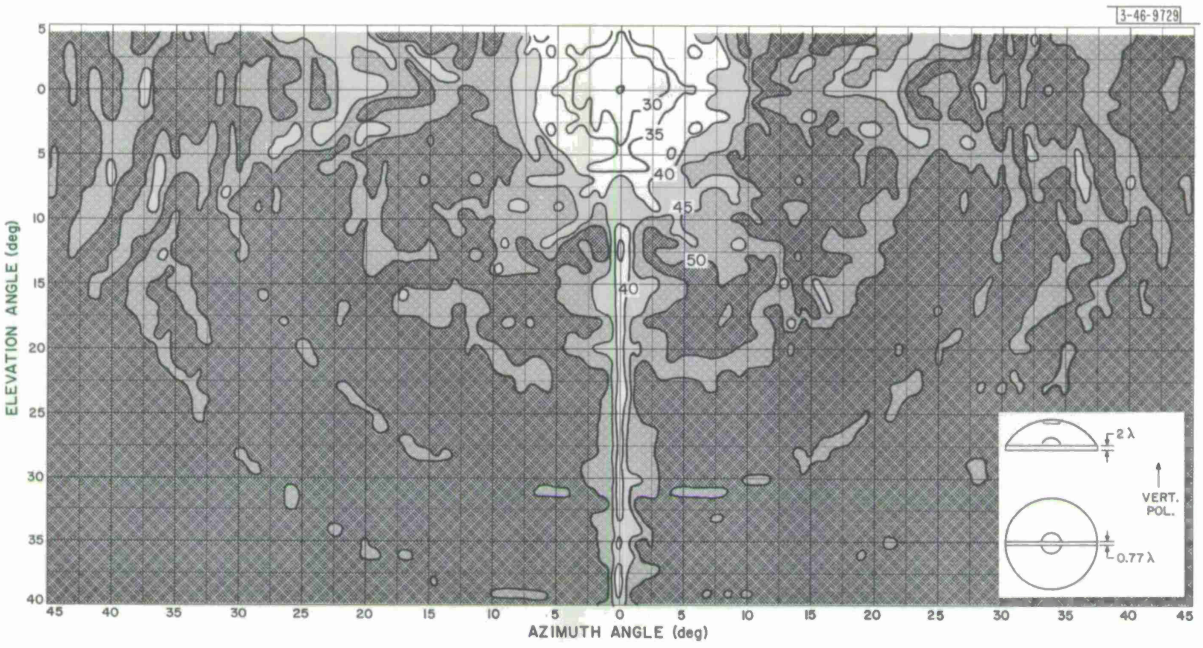

Fig. 10. Contour plot for 110-inch Cassegrainian dish with single support member (0.77λ × 2λ) oriented perpendicular to incident polarization.

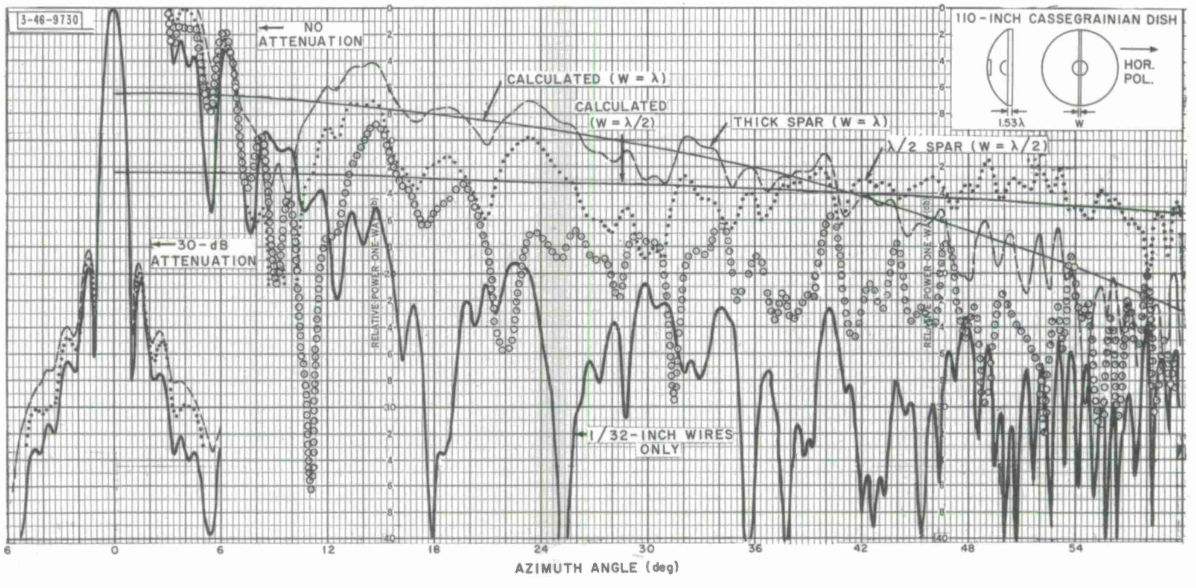

Fig. 11(a). Effect of single spar with perpendicular polarization (E-plane pattern).

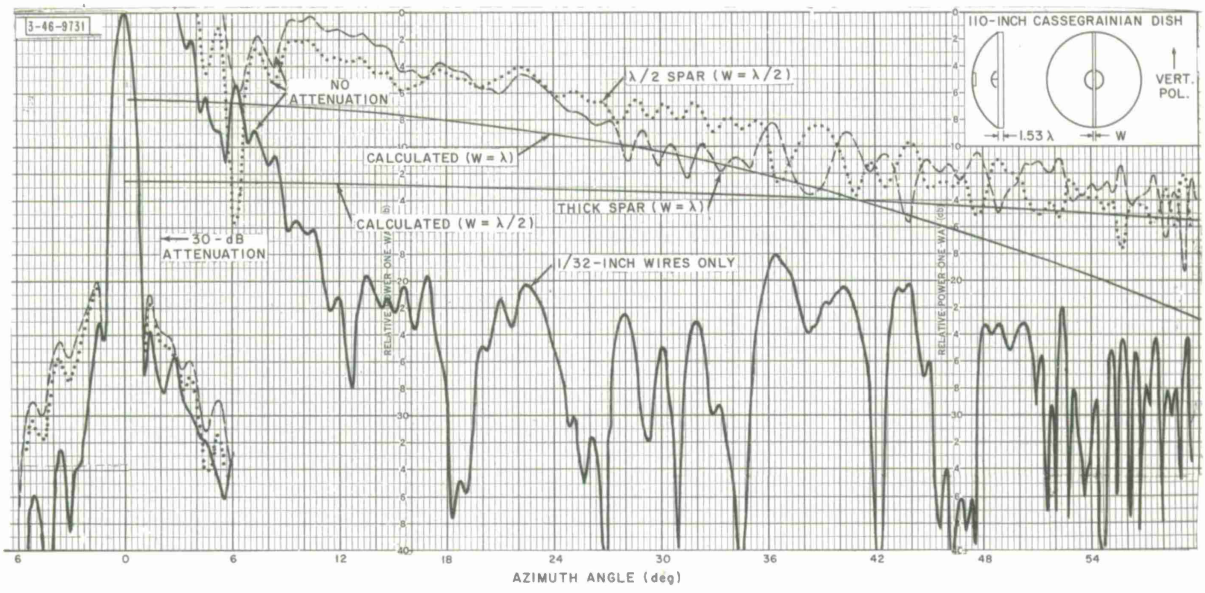

Fig. 11(b). Effect of single spar with parallel polarization (H-plane pattern).

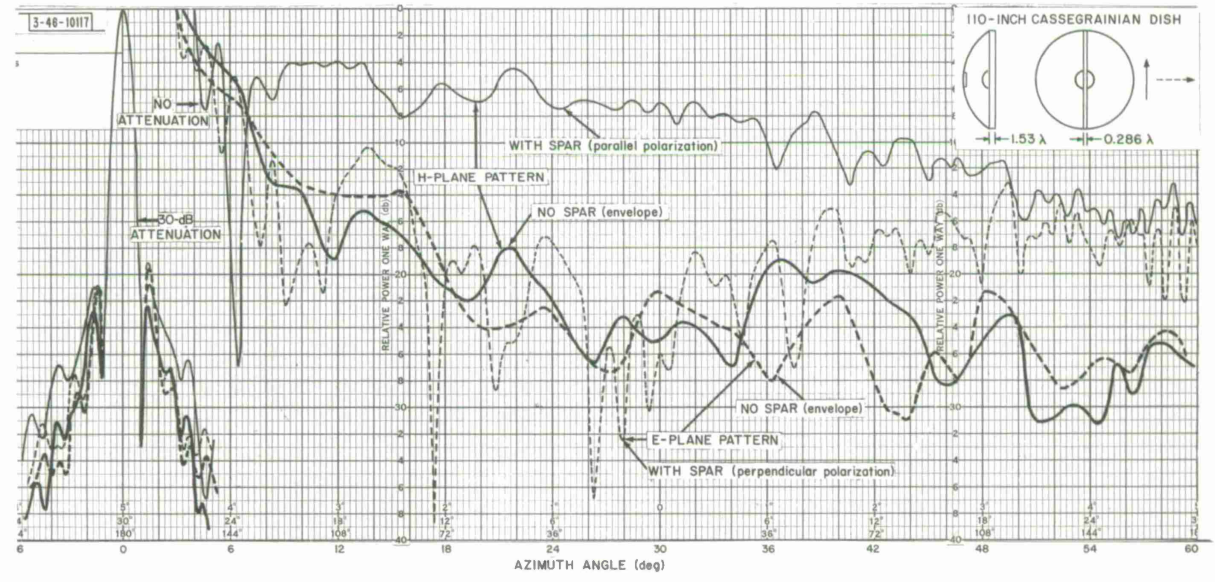

Fig. 11(c). Effect of single thin spar (w = 0.286 λ).

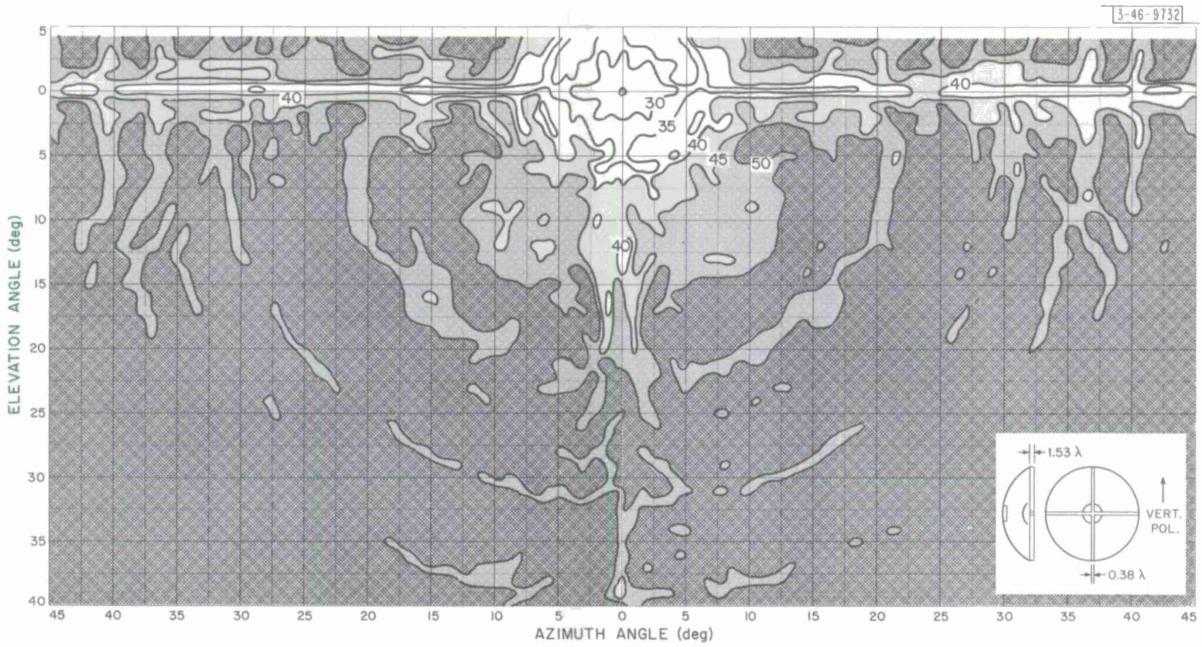

Fig. 12. Contour plot for 110-inch Cassegrainian dish with principal-plane spars (0.38 λ × 1.53 λ) at aperture.

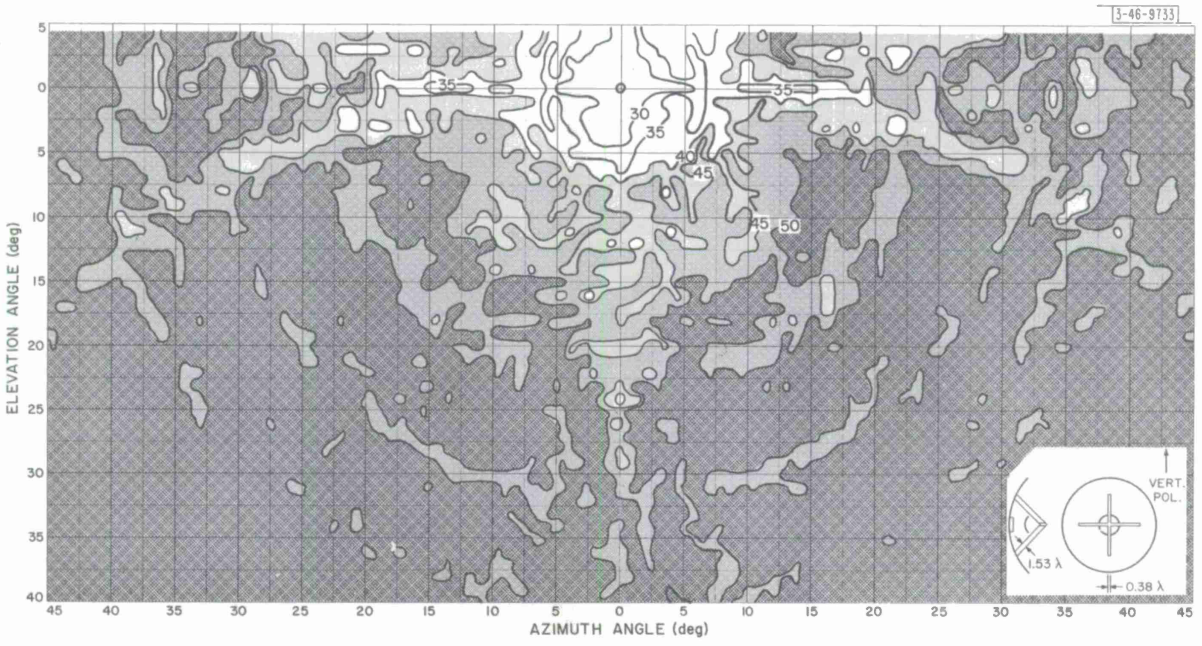

Fig. 13. Contour plot for 110-inch Cassegrainian dish with principal-plane spars (0.38 λ × 1.53 λ) inside aperture.

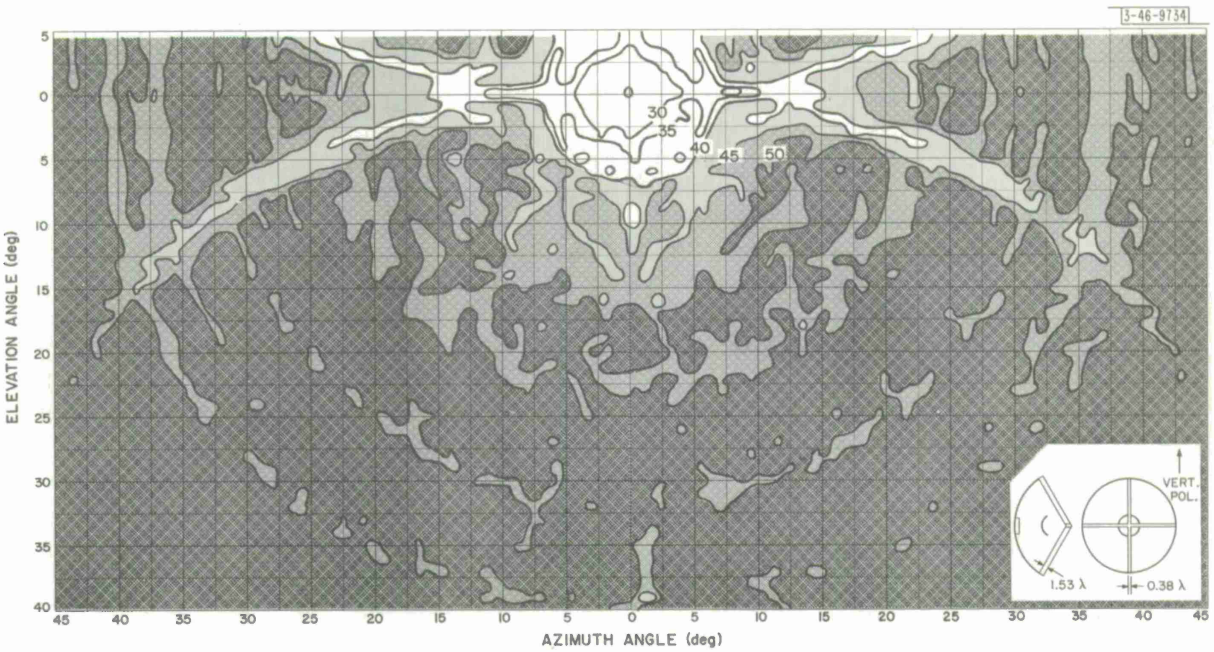

Fig. 14(a). Contour plot for 110-inch Cassegrainian dish with principal-plane spars (0.38 λ × 1.53 λ) outside aperture.

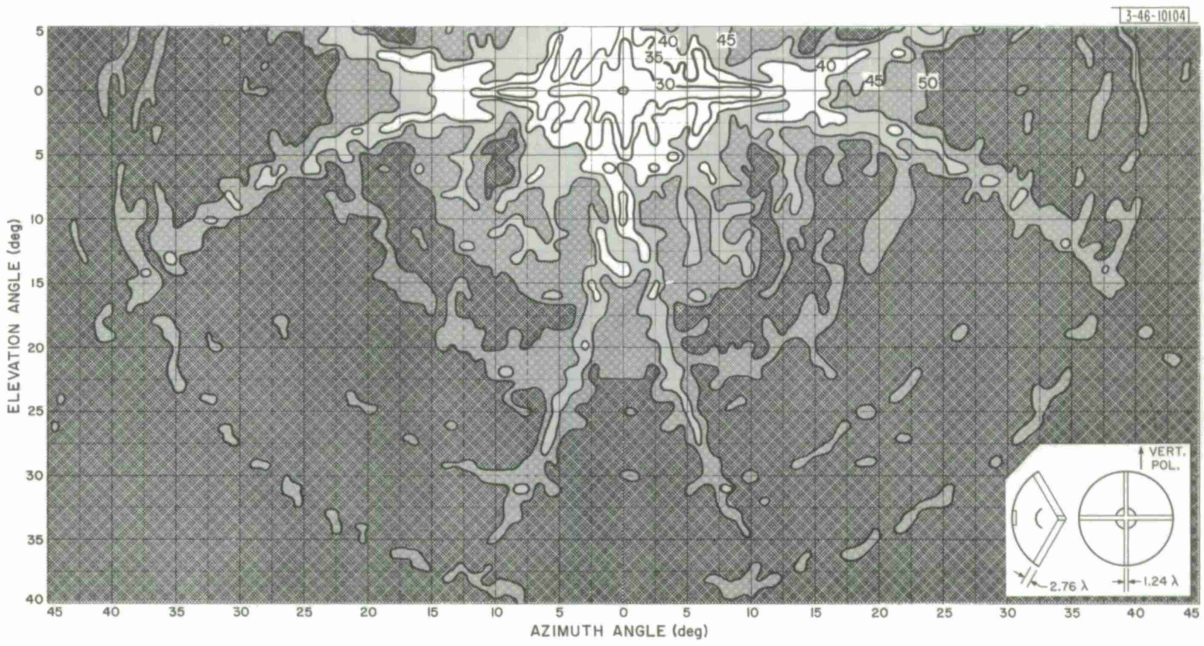

Fig. 14(b). Contour plot for 110-inch Cassegrainian dish with principal-plane spars (1.24 λ × 2.76 λ) outside aperture.

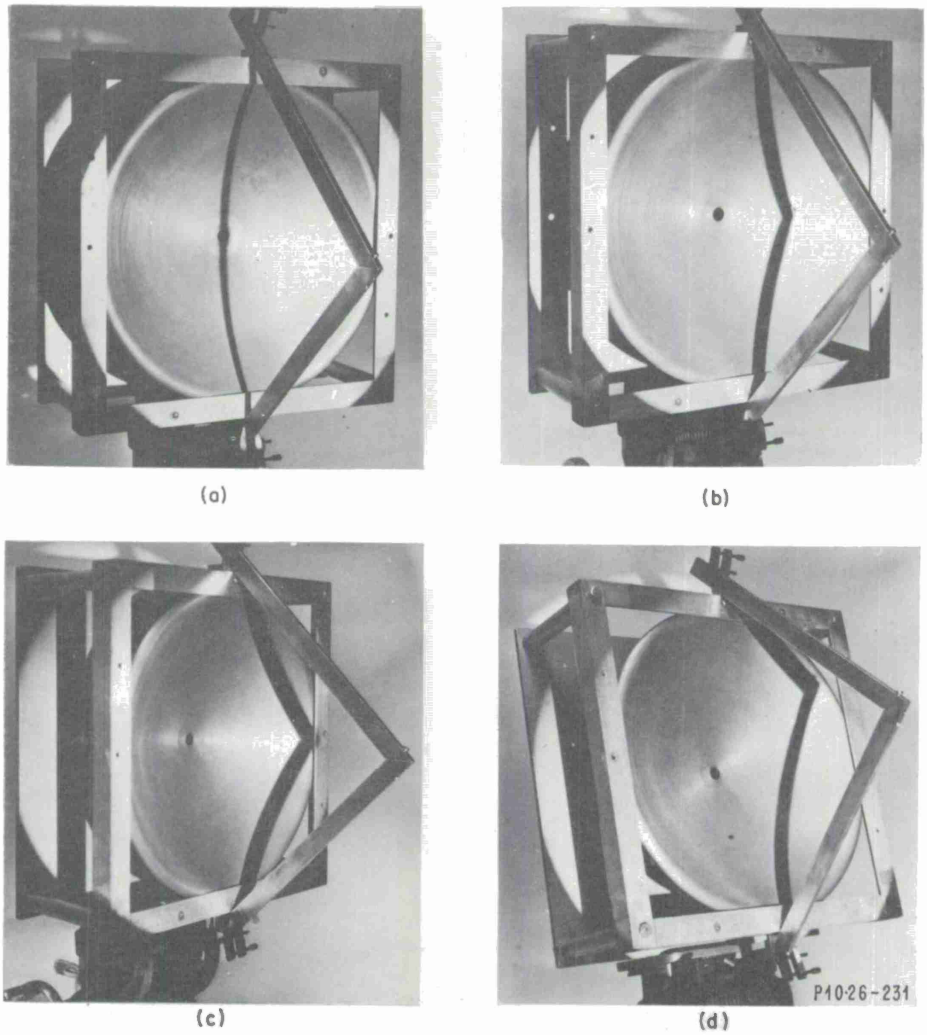

Fig. 15. Movement of shadowed area as function of off-axis illumination.

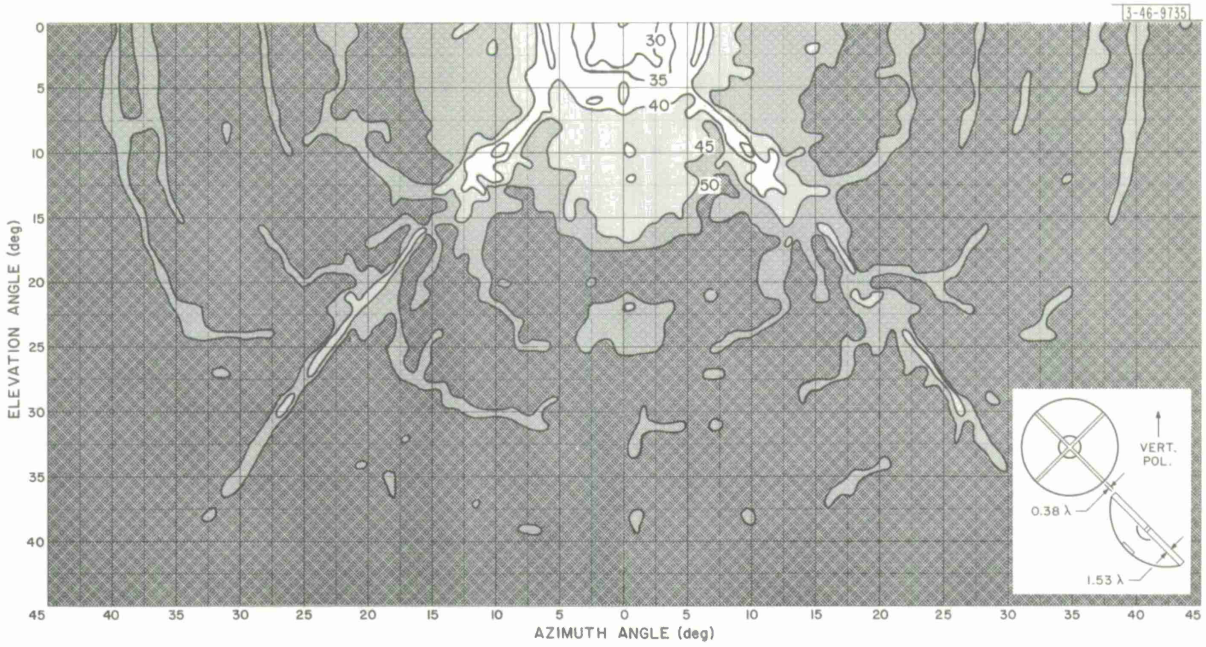

Fig. 16(a). Contour plot for 110-inch Cassegrainian dish with diagonal spars (0.38λ × 1.53λ) at aperture.

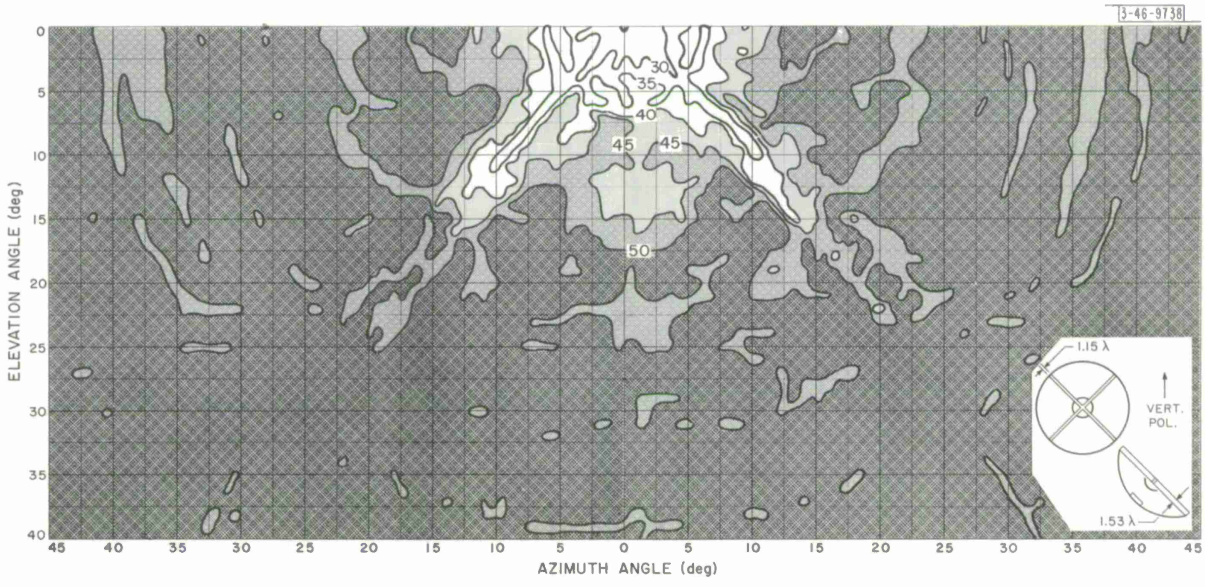

Fig. 16(b). Contour plot for 110-inch Cassegrainian dish with diagonal spars (1.15λ × 1.53λ) at aperture.

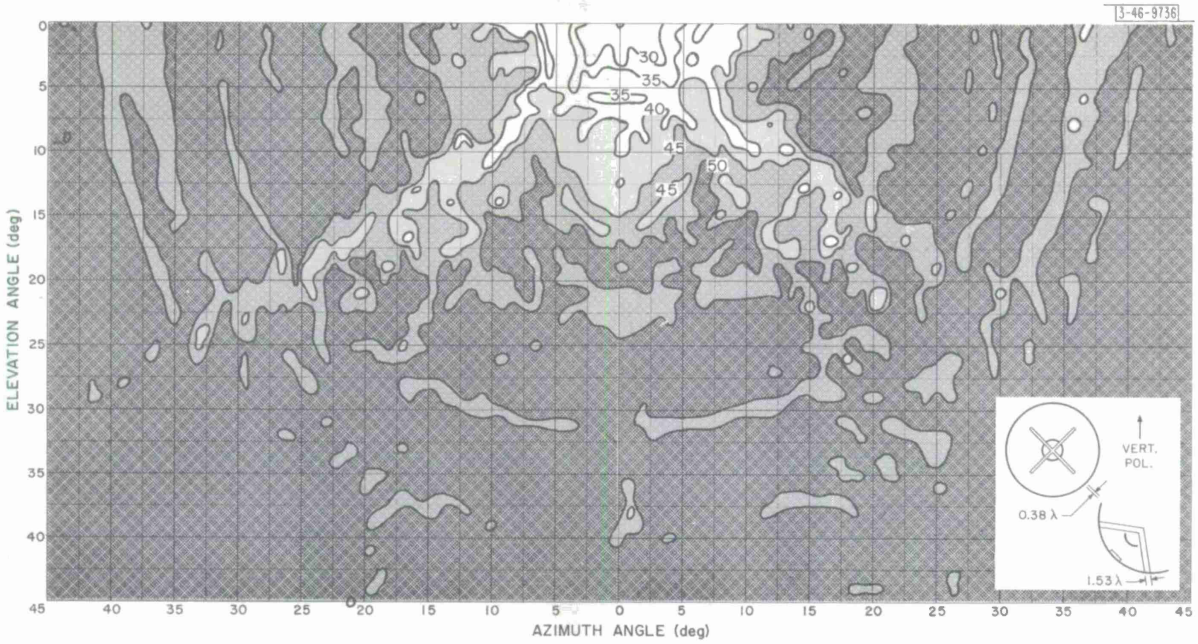

Fig. 17(a). Contour plot for 110-inch Cassegrainian dish with diagonal spars (0.38 λ × 1.53 λ) inside aperture.

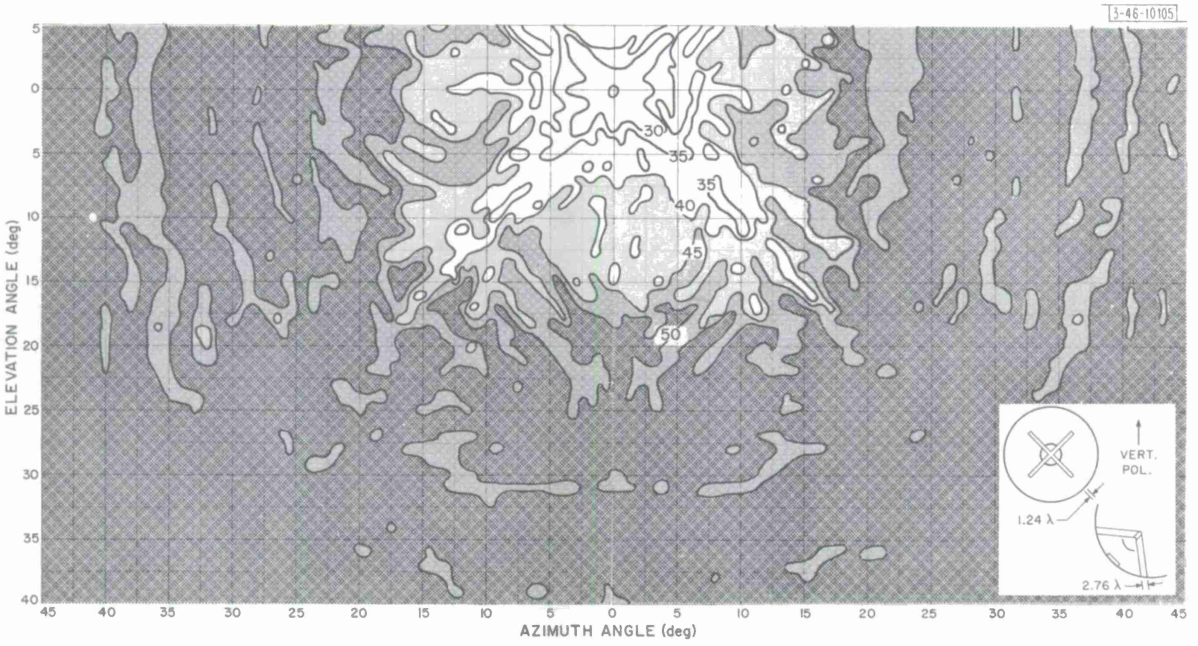

Fig. 17(b). Contour plot for 110-inch Cassegrainian dish with diagonal spars (1.24 λ × 2.76 λ) inside aperture.

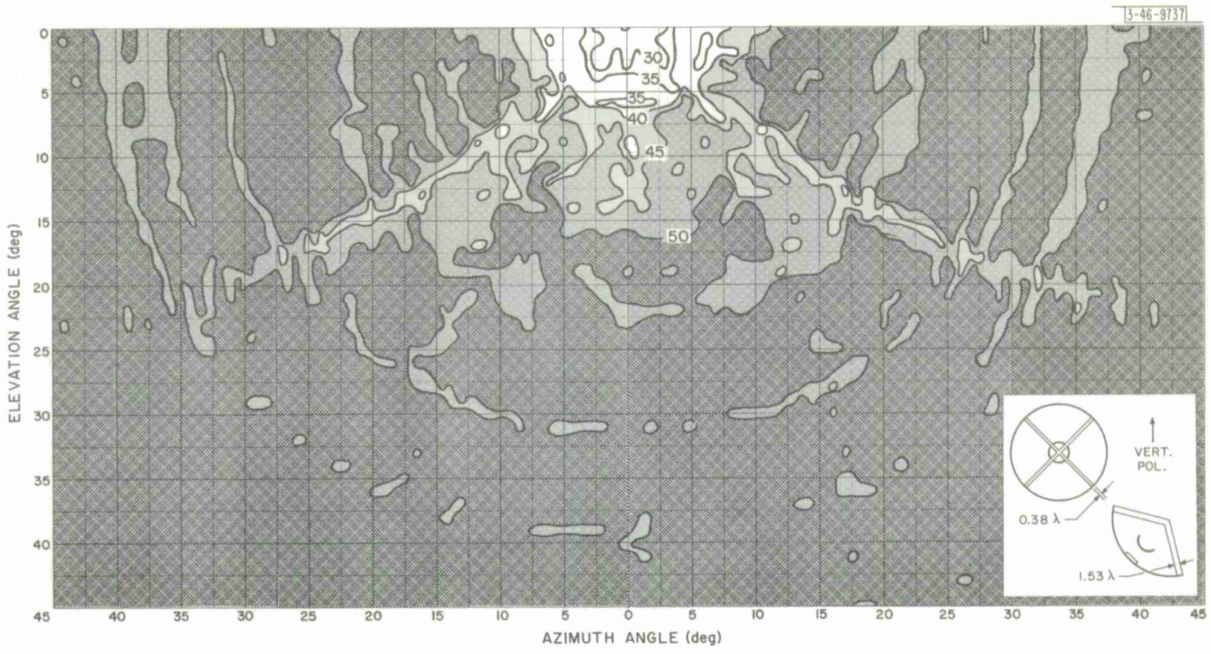

Fig. 18(a). Contour plot for 110-inch Cassegrainian dish with diagonal spars (0.38 λ × 1.53 λ) outside aperture.

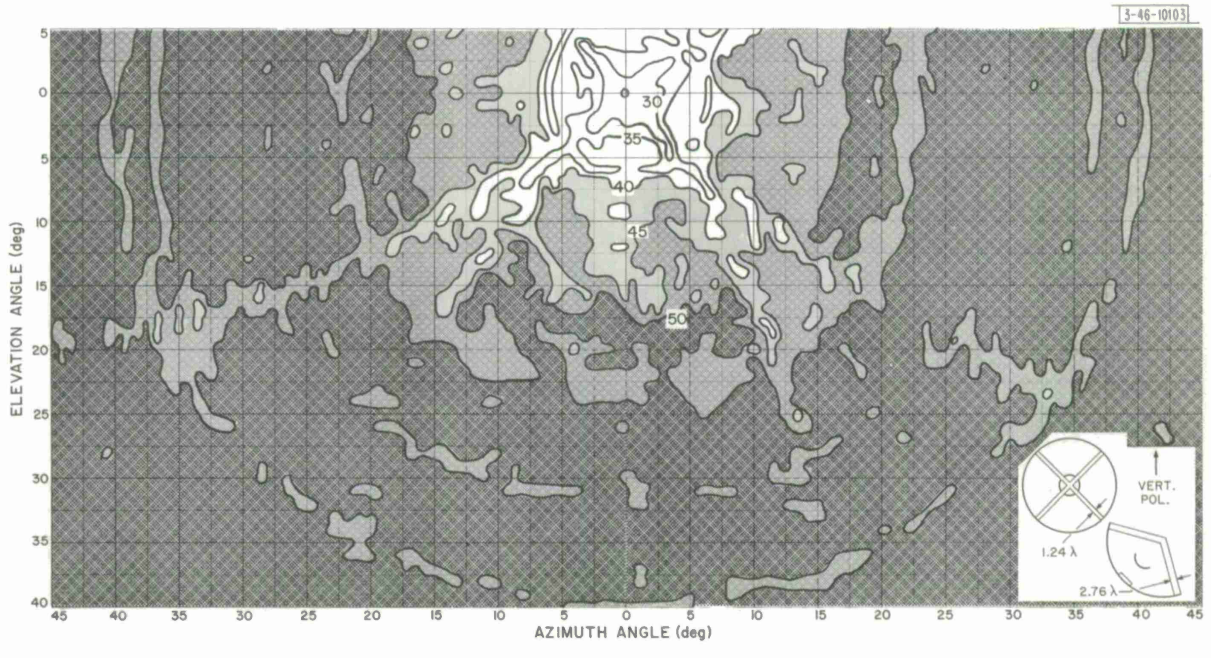

Fig. 18(b). Contour plot for 110-inch Cassegrainian dish with diagonal spars (1.24 λ × 2.76 λ) outside aperture.

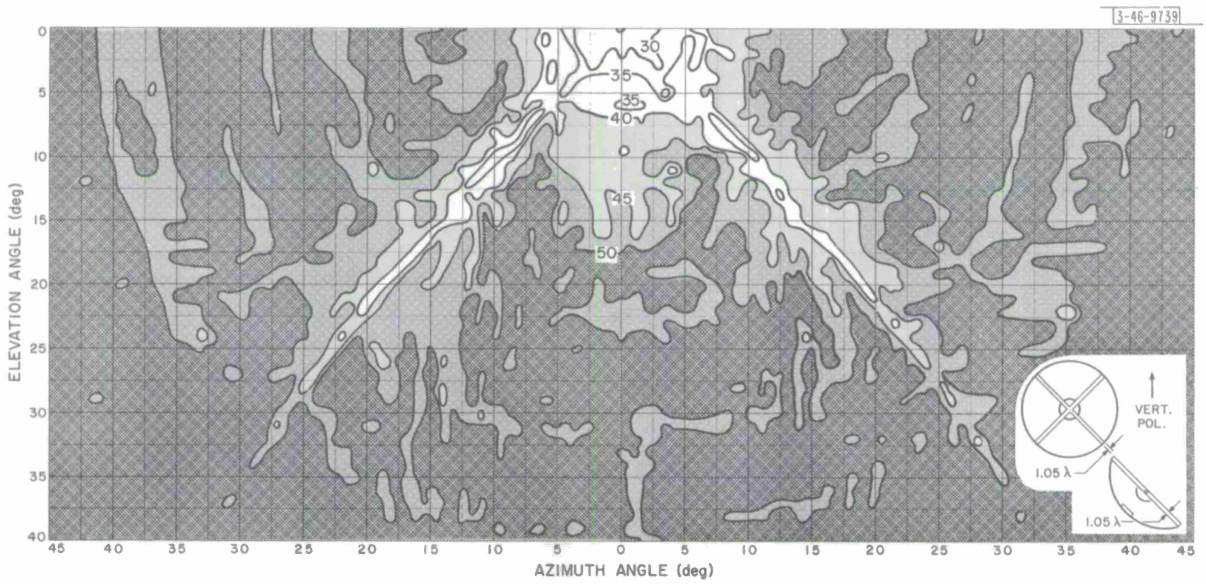

Fig. 19. Contour plot for 110-inch Cassegrainian dish with circular diagonal spars (1.05-λ diameter) at aperture.

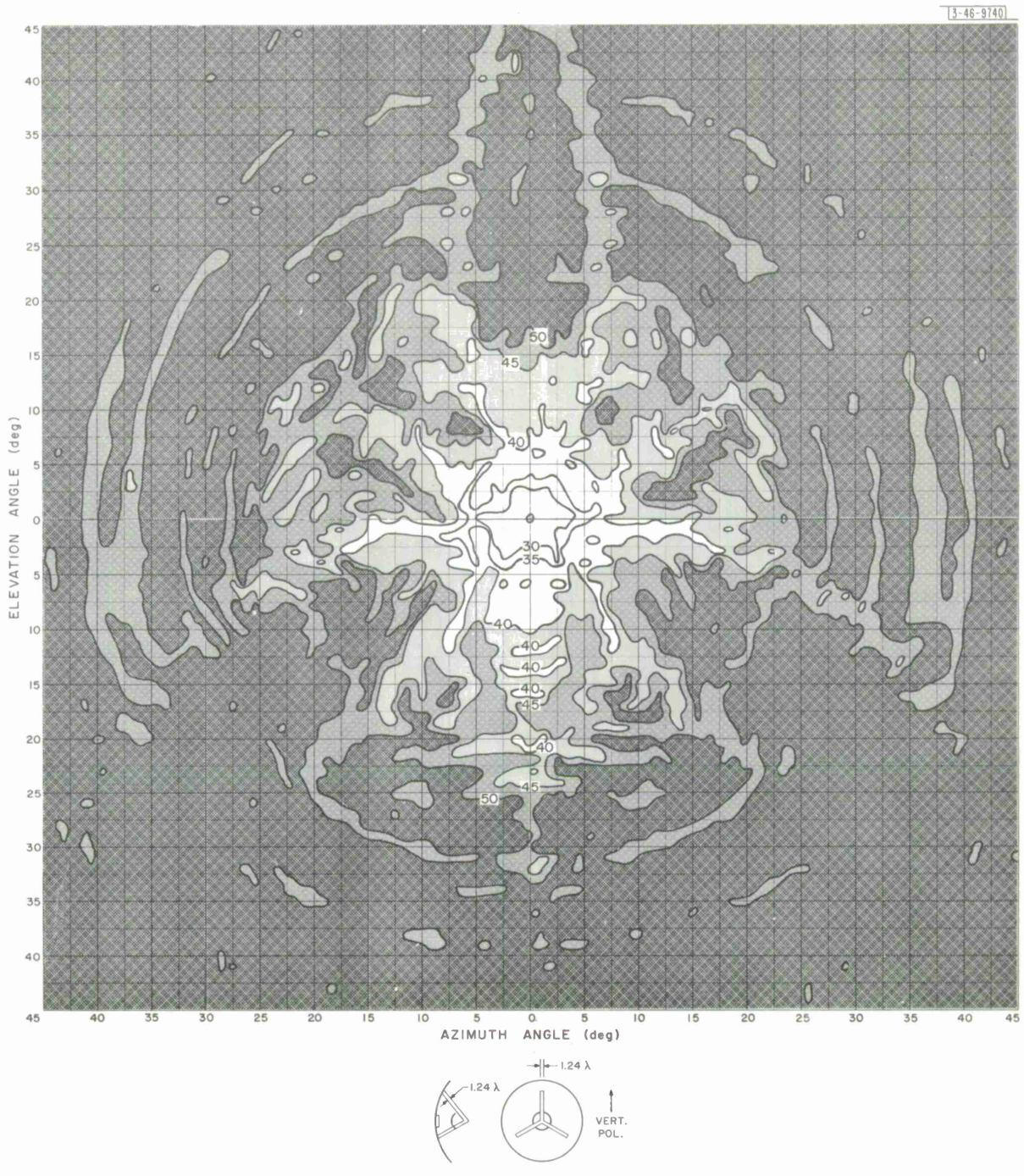

Fig. 20(a). Contour plot for 110-inch Cassegrainian dish with metallic tripod (1.24-λ diameter) inside aperture.

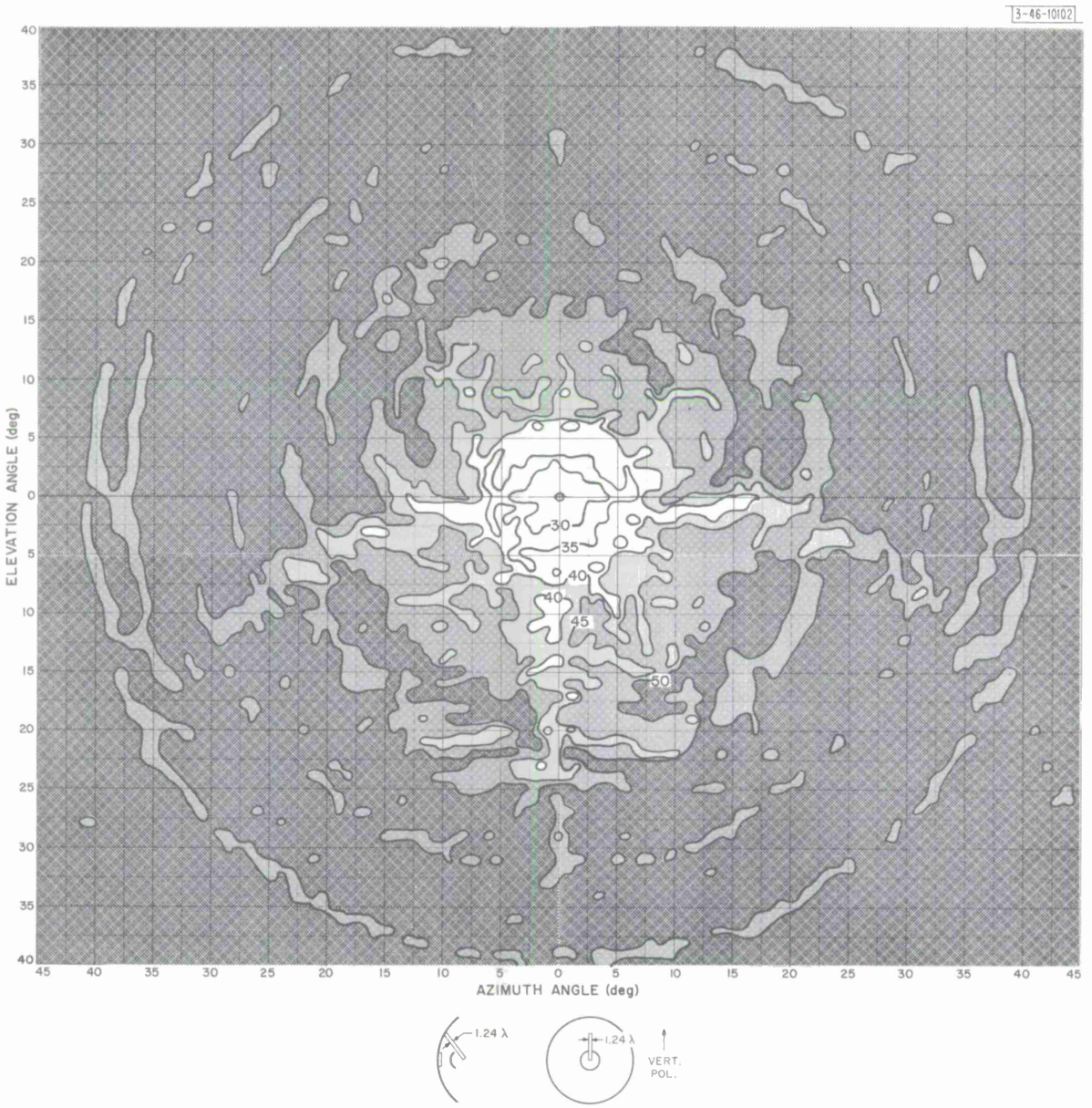

Fig. 20(b). Contour plot for 110-inch Cassegrainian dish with single tripod member.

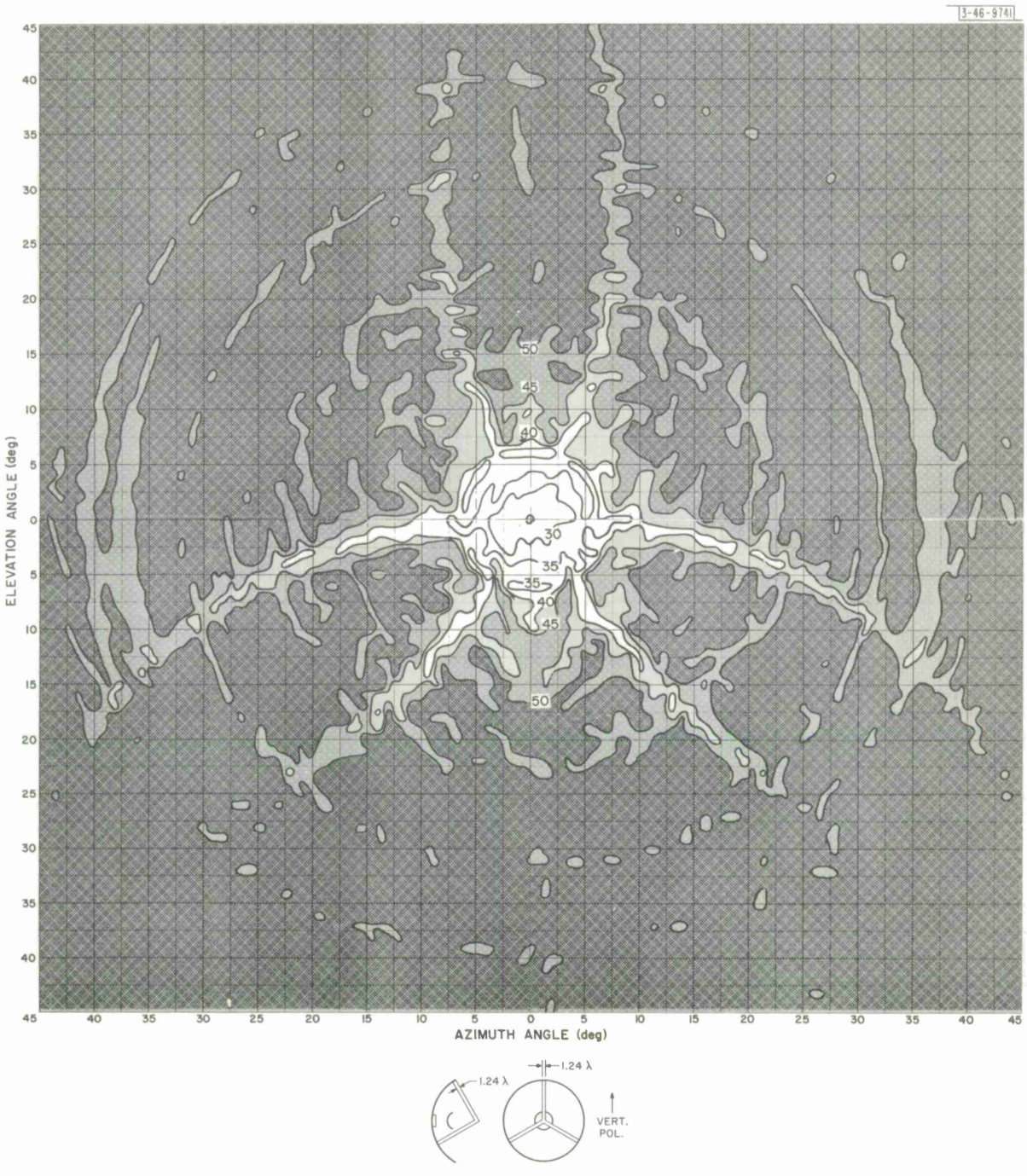

Fig. 21. Contour plot for 110-inch Cassegrainian dish with metallic tripod (1.24-λ diameter) outside aperture.

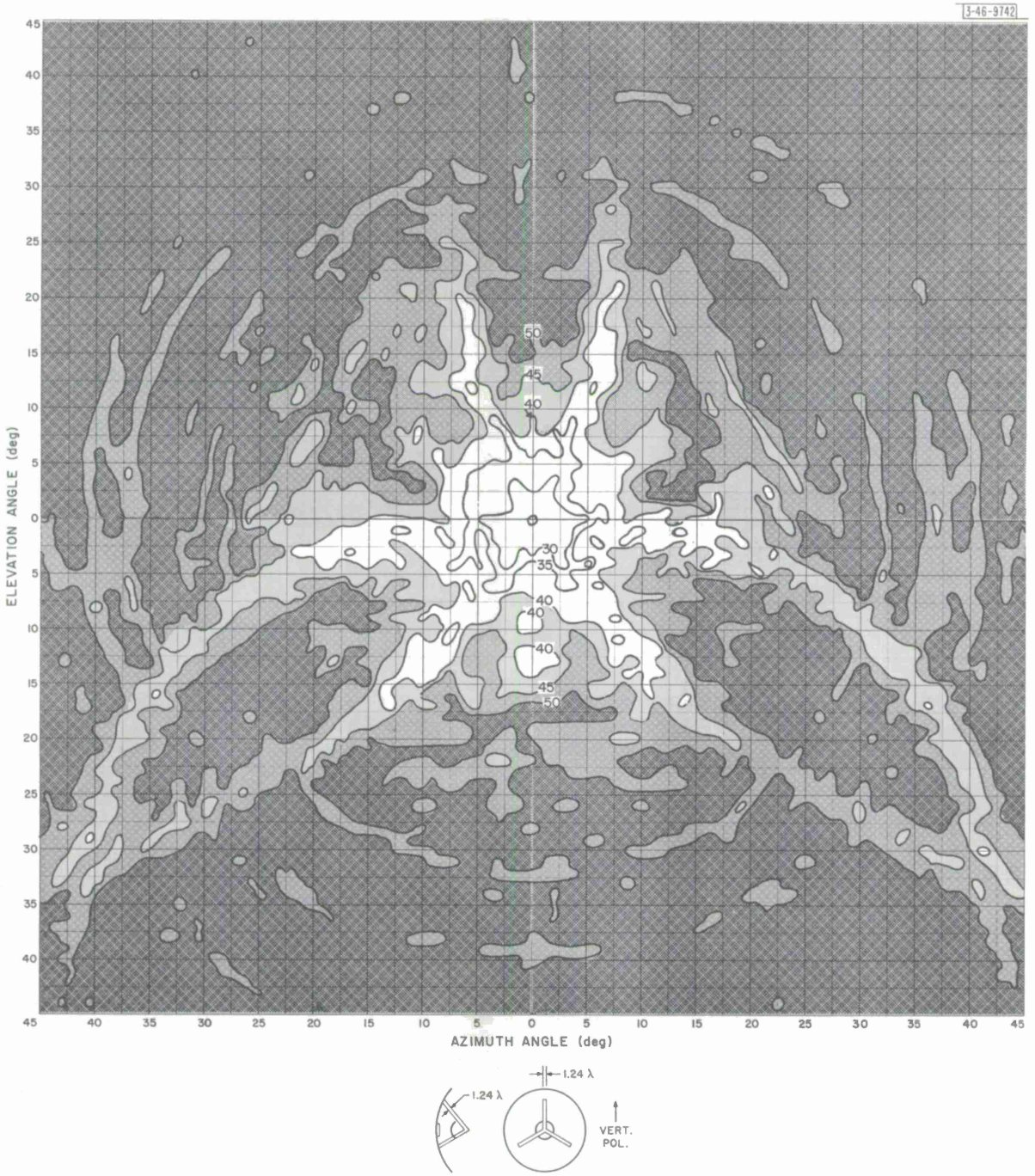

Fig. 22. Contour plot for 110-inch Cassegrainian dish with dielectric tripod (1.24-λ o.d., 1.05-λ i.d.) inside aperture.

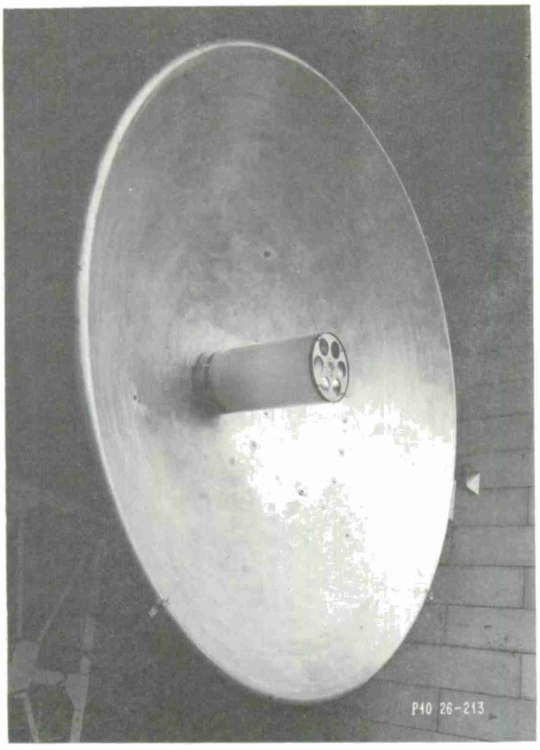

Fig. 23. Fiberglass cylinder supporting subreflector.

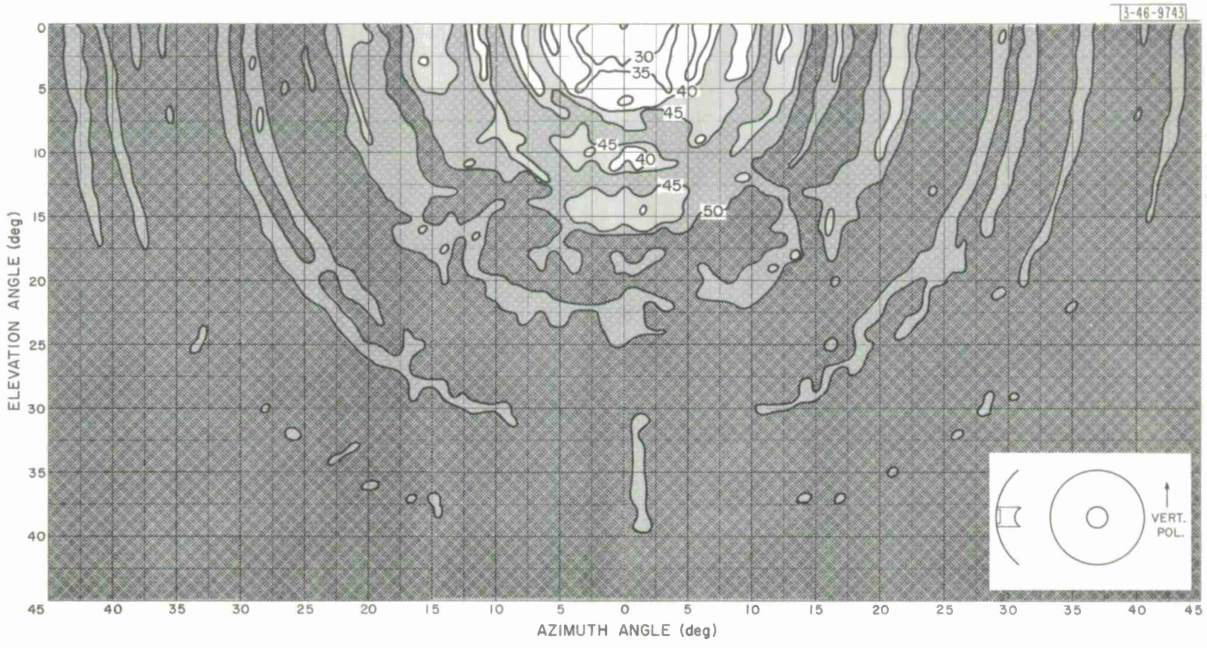

Fig. 24. Contour plot for 110-inch Cassegrainian dish with G-11 fiberglass cylinder (0.0175-λ wall) supporting subreflector.

DOCUMENT CONTROL DATA – R&D

(Security classification of title, body of abstract and indexing annotation must be entered when the overall report is classified)

1. ORIGINATING ACTIVITY *(Corporate author)* Lincoln Laboratory, M.I.T.	2a. REPORT SECURITY CLASSIFICATION Unclassified 2b. GROUP None

3. REPORT TITLE

Experimental Study of Subreflector Support Structures in a Cassegrainian Antenna

4. DESCRIPTIVE NOTES *(Type of report and inclusive dates)*

Technical Report

5. AUTHOR(S) *(Last name, first name, initial)*

Sheftman, Franklin I.

6. REPORT DATE	7a. TOTAL NO. OF PAGES	7b. NO. OF REFS
23 September 1966	36	7

8a. CONTRACT OR GRANT NO. AF 19(628)-5167 b. PROJECT NO. 649L c. d.	9a. ORIGINATOR'S REPORT NUMBER(S) Technical Report 416 9b. OTHER REPORT NO(S) *(Any other numbers that may be assigned this report)* ESD-TR-66-199

10. AVAILABILITY/LIMITATION NOTICES

Distribution of this document is unlimited.

11. SUPPLEMENTARY NOTES	12. SPONSORING MILITARY ACTIVITY
None	Air Force Systems Command, USAF

13. ABSTRACT

The effects of various support structures on the radiation patterns of a Cassegrainian antenna have been investigated experimentally. Detailed two-dimensional contour plots of the wide-angle radiation are presented primarily for support member dimensions up to about one wavelength. We show that the disturbing effects decrease rapidly for perpendicular polarization when the dimensions are decreased below $\lambda/2$. Furthermore, the on-axis geometrical shadowing due to the support members does not give the correct level and shape of the wide-angle radiation. Account must be taken of the polarization and orientation of the members relative to the antenna axis. The performance of dielectric members is shown to be generally poorer than that of metallic members. The alternative of supporting the subreflector with a thin-wall axial dielectric cylinder is shown to be electrically acceptable for thicknesses of the order of 0.01λ. The data presented should be useful in designing and evaluating various types of support structures for Cassegrainian and front-fed reflectors.

14. KEY WORDS

subreflector support structures
antenna feed supports
Cassegrainian antenna
scattering
sidelobes
radiation patterns
polarization

Printed by
United States Air Force
L. G. Hanscom Field
Bedford, Massachusetts